JOURNAL OF VIROLOGY, Sept. 2008, p. 8797–8811 Vol. 82, No. 17
0022-538X/08/$08.00+0 doi:10.1128/JVI.00592-08
Copyright © 2008, American Society for Microbiology. All Rights Reserved.

Protein Kinase A-Dependent Step(s) in Hepatitis C Virus Entry and Infectivity▽

Michelle J. Farquhar,[1] Helen J. Harris,[1] Mandy Diskar,[2] Sarah Jones,[3] Christopher J. Mee,[1] Søren U. Nielsen,[4] Claire L. Brimacombe,[1] Sonia Molina,[5] Geoffrey L. Toms,[4] Patrick Maurel,[5] John Howl,[3] Friedrich W. Herberg,[2] Sven C. D. van IJzendoorn,[6] Peter Balfe,[1]* and Jane A. McKeating[1]

Hepatitis C Research Group, Division of Immunity and Infection, University of Birmingham, Vincent Drive, Birmingham, United Kingdom[1]; University of Kassel, Department of Biochemistry, Heinrich Plett Str. 40, D-34132 Kassel, Germany[2]; Molecular Pharmacology Research Group, Research Institute in Healthcare Science, University of Wolverhampton, Wulfruna Street, Wolverhampton, United Kingdom[3]; Liver Research Group, School of Clinical Medical Sciences, The Medical School, Newcastle upon Tyne, United Kingdom[4]; Inserm U632, Hepatic Physiopathology, 191 Route de Mende, 34293 Montpellier Cedex 5, France[5]; and Department of Cell Biology/Membrane Cell Biology, University Medical Centre Groningen, University of Groningen, Groningen, The Netherlands[6]

Received 17 March 2008/Accepted 16 June 2008

Viruses exploit signaling pathways to their advantage during multiple stages of their life cycle. We demonstrate a role for protein kinase A (PKA) in the hepatitis C virus (HCV) life cycle. The inhibition of PKA with H89, cyclic AMP (cAMP) antagonists, or the protein kinase inhibitor peptide reduced HCV entry into Huh-7.5 hepatoma cells. Bioluminescence resonance energy transfer methodology allowed us to investigate the PKA isoform specificity of the cAMP antagonists in Huh-7.5 cells, suggesting a role for PKA type II in HCV internalization. Since viral entry is dependent on the host cell expression of CD81, scavenger receptor BI, and claudin-1 (CLDN1), we studied the role of PKA in regulating viral receptor localization by confocal imaging and fluorescence resonance energy transfer (FRET) analysis. Inhibiting PKA activity in Huh-7.5 cells induced a reorganization of CLDN1 from the plasma membrane to an intracellular vesicular location(s) and disrupted FRET between CLDN1 and CD81, demonstrating the importance of CLDN1 expression at the plasma membrane for viral receptor activity. Inhibiting PKA activity in Huh-7.5 cells reduced the infectivity of extracellular virus without modulating the level of cell-free HCV RNA, suggesting that particle secretion was not affected but that specific infectivity was reduced. Viral particles released from H89-treated cells displayed the same range of buoyant densities as did those from control cells, suggesting that viral protein association with lipoproteins is not regulated by PKA. HCV infection of Huh-7.5 cells increased cAMP levels and phosphorylated PKA substrates, supporting a model where infection activates PKA in a cAMP-dependent manner to promote virus release and transmission.

Hepatitis C virus (HCV) is an enveloped positive-stranded RNA virus and the sole member of the genus *Hepacivirus* within the *Flaviviridae*. Approximately 170 million individuals are infected with HCV worldwide, and the majority are at risk for developing serious progressive liver disease. The HCV RNA genome of approximately 9.6 kb encodes a polyprotein of around 3,000 amino acids, which is cleaved by viral and cellular proteases to generate the structural and nonstructural (NS) proteins. The amino terminus of the polyprotein sequence contains the structural proteins including the core, the envelope glycoproteins (GPs) E1 and E2, and p7. The NS proteins including NS2 through NS5 are located at the carboxy terminus of the polyprotein. Much of our current understanding of HCV replication has been gained through the use of genomic replicons (reviewed in reference 7). The recent development of an infectious system allowing the generation of HCV particles in cell culture (HCVcc) has enabled the complete viral life cycle to be explored (63, 99, 110).

Viruses utilize signaling pathways of their target cells to their advantage during multiple steps of their life cycle including entry, internalization, replication, and release (21, 24, 80, 87, 91). The lateral movement of human immunodeficiency virus type 1 (HIV-1) and coxsackie B viruses along the membrane of target cells prior to entry is dependent upon signaling pathways that modulate the cytoskeleton to facilitate receptor attachment and particle internalization (26, 59). Viral replication exploits intracellular signaling pathways; for example, herpes simplex virus expression is dependent on protein kinase A (PKA) (103), HIV transcription and replication are increased in response to the synergistic activation of PKA and protein kinase C (PKC) (85), and vaccinia virus replication requires the mitogen-activated protein kinase (MAPK) pathway (3). Signaling molecules that play important roles in the secretory pathway are utilized by viruses during particle assembly and release (76).

Recent advances in methods to study HCV entry have demonstrated the involvement of at least three host cell molecules: the tetraspanin CD81 (82, 107), scavenger receptor class B member I (SR-BI) (8, 41, 88), and the tight-junction (TJ) protein claudin-1 (CLDN1) (34, 72, 104, 109). CD81 is a mem-

* Corresponding author. Mailing address: Hepatitis C Research Group, Division of Immunity and Infection, University of Birmingham, Vincent Drive, Birmingham B15 2TT, United Kingdom. Phone: (44) 121 414 8174. Fax: (44) 121 414 3599. E-mail: p.balfe@bham.ac.uk.

▽ Published ahead of print on 25 June 2008.

ber of the tetraspanin family of expressed membrane proteins that are reported to influence multiple cellular properties including adhesion, morphology, and proliferation (reviewed in reference 60). The intracellular domain of CD81 associates with the signaling enzymes phosphatidylinositol 4-kinase and PKC (9, 108). SR-BI expression within the liver is regulated by cyclic AMP (cAMP)-dependent PKA phosphorylation of PDZK1, and its transcytosis in polarized MDCK cells requires PKA (18, 77). Many cellular signaling proteins are involved in TJ formation, and the recently identified role of CLDN1 in HCV entry highlights a route by which the virus could modulate target cell signaling to its advantage (6, 57, 62).

In this study, we investigated a role for protein kinase signaling in HCV infection by examining the effect of kinase inhibitors and antagonists on viral entry, replication, and the release of infectious particles. Inhibition of PKA led to a redistribution of CLDN1 from the plasma membrane and a concomitant reduction in viral entry, confirming the importance of CLDN1 localization at the plasma membrane for viral receptor activity. In addition, we reveal a role for PKA in regulating the infectivity of cell-free virus particles. Finally, we demonstrate increased levels of cAMP and PKA substrates in HCV-infected cells, supporting a model where infection activates PKA in a cAMP-dependent manner as a mechanism to promote the infectivity of extracellular virus and to aid viral transmission.

MATERIALS AND METHODS

Cell lines, antibodies, and reagents. Huh-7.5 cells (provided by Charles Rice, The Rockefeller University, New York, NY) (14), Huh-7 cells (provided by Frank Chisari, Scripps Research Institute), Hep3B, and 293T cells (purchased from the American Type Culture Collection) were propagated in Dulbecco's modified Eagle medium (DMEM) supplemented with 10% fetal bovine serum (FBS) and 1% nonessential amino acids (Invitrogen, CA). 293T cells transduced to express CLDN1 (43) were propagated in 10% FBS–DMEM. Primary human hepatocytes were isolated and cultured as previously reported (81). All cells were grown in a humidified atmosphere at 37°C in 5% CO_2.

The primary antibodies used were anti-CLDN1 JAY.8 (Invitrogen, CA), anti-CLDN1 1C5-D9 (Novus, CO), anti-CD81 M38 (Fedor Berditchevski, University of Birmingham, Birmingham, United Kingdom), anti-SR-BI 25 (BD Biosciences, NJ), anti-NS5A 9E10 (C. Rice, Rockefeller University), and anti-phospho-Ser/Thr PKA substrate (p-PKAs) (Cell Signaling Technology, Inc., MA). Secondary labeled antibodies were obtained from Invitrogen: Alexa Fluor 488 goat anti-mouse immunoglobulin G (IgG) Alexa Fluor 488 goat anti-rabbit IgG, and Alexa Fluor 633 goat anti-mouse IgG. Horseradish peroxidase (HRP)-conjugated sheep anti-mouse and donkey anti-rabbit secondary antibodies were obtained from GE Healthcare.

Kinase inhibitor and antagonists were obtained from the following sources: Ro-31-8220 and H89 from Calbiochem; Rp-cAMPS (adenosine 3′,5′-cyclic phosphorothioate) and Rp-8-Br-cAMPS (Janet Lord, University of Birmingham, Birmingham, United Kingdom) from BioLog; myristoylated protein kinase I (14–22) amide (myrPKI) from Biomol International; and forskolin (FK), mitogen-activated protein kinase 1 (MEK1), PD98059, U0126, and SB203580 from Sigma. Green fluorescent protein (GFP)–A-kinase-anchoring protein (AKAP) in silico (AKAP-IS)–V5 (His), and GFP-Scrambled-V5 (His) were kindly donated by John Scott (Howard Hughes Medical Center).

Genesis of virus and infections. Cell culture-derived virus particles, J6/JFH and JFH-1, were generated as previously described (63). Briefly, using the Megascript T7 kit (Ambion, Austin, TX), RNA was transcribed in vitro from full-length genomes and electroporated into Huh-7.5 cells. High-titer stocks were generated by serial passage through naïve Huh-7.5 cells (34). Supernatants were collected at 72 and 96 h postinfection, pooled, and stored at −80°C. Infected cells were detected by methanol fixation and staining for NS5A using the anti-NS5A 9E10 antibody; bound antibody was detected with an Alexa 488-conjugated anti-mouse IgG and quantified by flow cytometry.

Pseudoviruses expressing luciferase or enhanced GFP (eGFP) reporters were generated by the following protocols. 293T cells were transfected with a 1:1 ratio of plasmids encoding HIV provirus expressing luciferase and HCV strain H77 E1E2 envelope GPs (HCVpp-H77), MLV GP (MLVpp), or empty vector (Env-pp), as previously described (49). Alternatively, 293T cells were cotransfected with plasmids encoding HIV provirus expressing eGFP (CSGW) (11), HIV Gag-Pol, and HCV strain JFH GPs or empty vector in a 1:1:4 ratio as previously described (36). Supernatants were harvested 48 h posttransfection, pooled, and filtered. Infection was quantified by measuring cellular eGFP expression by flow cytometry or luciferase activity in a luminometer (Berthold Centro LB 960). Specific infectivity was calculated by subtracting the mean Env-pp signal from the HCVpp or MLVpp signal. Relative infectivity was calculated as a percentage of untreated cells and presented as the standard error of the mean, where the mean infection value of replicate untreated cell wells was defined as 100%.

Effect of kinase inhibitor/activators on HCV entry. Various target cells were seeded at 1.5×10^4 cells/cm^2, subjected to a 3-h serum starvation the following day, and incubated with inhibitors/agonists diluted in serum-free DMEM for 1 h. HCVcc/HCVpp-containing medium was added to target cells and incubated for 1 h and 6 h, respectively, unbound virus/inhibitors were removed by washing, and the medium was replaced with 3% FBS–DMEM. After 48 and 72 h for HCVcc and HCVpp, respectively, infection was assessed as described above.

Effect of kinase inhibitor/activators on cell-free virus infectivity. To evaluate the level of infectious virus released from J6/JFH- and JFH-1-infected cultures, cells were seeded at 6×10^4 cells/cm^2 in 48-well plates, serum starved for 3 h the following day, and incubated with modulators of PKA for 1 h. Cells were washed extensively, and cell-free medium was collected for the quantification of infectious virus or HCV RNA.

To quantify extracellular virus infectivity, the collected medium was allowed to infect naïve Huh-7.5 target cells at various dilutions for 1 h at 37°C. Intracellular virus was released by three rapid freeze-thaw cycles of infected cells, and the clarified lysate was used to infect Huh-7.5 cells. Viral infection was detected after 48 h by staining for NS5A, and antigen-positive cells were enumerated on a Nikon TE2000 apparatus. Infectivity is defined as the number of infected cells or units per ml (IU/ml) and expressed relative to control untreated cells as described above.

BRET assay to investigate PKAI and PKAII dynamics in living cells. Bioluminescence resonance energy transfer (BRET) experiments were performed as previously described (29, 83). In brief, 1.5×10^4 Huh-7.5 cells were seeded per well of a white 96-well microplate (Nunc, Thermo Fisher, Denmark) and transfected with 0.2 μg of plasmids encoding PKA type I (PKAI) (GFP2-C3-hCα [Perkin Elmer, Massachusetts] [83] and *Renilla* luciferase [Rluc]-N2-hRIα) and PKAII (GFP2-C3-hCα and Rluc-N2-hRIIα) sensors the following day. At 48 h posttransfection, the cells were washed with phosphate-buffered saline (PBS) and incubated with antagonists for 1 h. Subsequently, the cells were stimulated with agonists in the presence of either 50 μM FK (Sigma, United Kingdom) and 500 μM 3-isobutyl-1-methylxanthine (IBMX; Sigma, United Kingdom) or FK alone (10 μM) for 30 min in the continued presence of antagonists or were mock treated with PBS (control). To quantify BRET, the medium was removed, 50 μl of substrate (DeepBlueC in PBS) was added per well, and Rluc/GFP2 light emission was detected using a Fusionα-FP microplate reader (Perkin-Elmer) (84). The light output was measured consecutively (read time, 1 s; gain, 25) using filters at a 410-nm wavelength (±80-nm bandpass) for the donor and at a 515-nm wavelength (±30-nm bandpass) for the acceptor. The emission from nontransfected (NT) cells was subtracted, and the BRET signal was calculated as follows: [emission (515 nm) − NT cells (515 nm)]/[emission (410 nm) − NT cells (410 nm)]. Control measurements with cells expressing Rluc were included in each experiment to determine the background BRET signal. Statistical analyses were performed with GraphPad Prism, version 4 (GraphPad Software, San Diego, CA).

Imaging of CD81, CLDN1, SR-BI, and PKA substrate(s). Naïve and JFH-1-infected Huh-7.5 cells were seeded onto borosilicate glass coverslips at a density of 1.5×10^4 cells/cm^2. The following day, cells were serum starved for 3 h, incubated with H89 or FK for 1 h, and, dependent on the antibody to be used, fixed in 1% paraformaldehyde (M38) or methanol (remaining antibodies). Cells were permeabilized for 30 min in 0.1% saponin–1% bovine serum albumin (BSA) in PBS and incubated with antibodies specific for CD81 (M38), SR-BI (anti-ClaI), CLDN1 (1C5-D9), phospho-Ser/Thr PKA substrate (p-PKAs), or NS5A (9E10). Cells were washed three times in PBS-saponin-BSA before the addition of the relevant secondary Alexa Fluor-conjugated antibodies in PBS-saponin-BSA for 1 h at room temperature. Cells were washed three times in PBS-saponin-BSA before counterstaining with 4′,6′-diamidino-2-phenylindole (DAPI) (Invitrogen) in PBS for 5 min. Coverslips were mounted onto glass slides (ProLong Gold antifade; Invitrogen, CA), and images were analyzed by laser scanning confocal microscopy (Zeiss LSM510) with a 63× water immersion objective.

FRET to quantify CLDN1-CD81 association. Huh-7.5 cells were transduced with TRIP viruses encoding AcGFP.CD81 and DsRed.CLDN1 (43) and grown on 22-mm-diameter borosilicate glass coverslips. Images were collected using a Meta Head laser scanning confocal microscope (Zeiss, model LSM510), and areas of protein colocalization (defined as 100% pixel overlap) were identified using the colocalization finder plugin (42) and Image J software (W. S. Rasband, U.S. National Institutes of Health, Bethesda, MD [http://rsb.info.nih.gov/ij/]). Proteins within regions of interest were assessed for fluorescence resonance energy transfer (FRET) as described previously (43). Briefly, the percentage of fields where FRET occurs is an indicator of the frequency of protein-protein associations. The efficiency of FRET was obtained by measuring the fluorescence intensities of the donor fluorophore before and after photobleaching of the acceptor fluorophore (10, 105). To minimize spectral bleedthrough, we utilized the Meta Head function of the microscope at the following wavelengths: excitation wavelength of 488 nm and emission wavelength of 520 nm for AcGFP and excitation wavelength of 561 nm and emission wavelength of 600 nm for DsRed. Statistical analyses were performed using Fisher's exact test with correction for multiple sampling where appropriate.

Immunoprecipitation and Western blotting. Huh-7.5 cells (seeded the preceding day at 1.5×10^4 cells/cm^2) were harvested in lysis buffer (PBS, 1% Triton X-100, 0.1% sodium deoxycholate, 0.1% sodium dodecyl sulfate [SDS]) containing protease (Complete; Roche, United Kingdom) and phosphatase (PhoStop; Roche, United Kingdom) inhibitors. Cell lysates were clarified by centrifugation (20,000 $\times$ *g* for 30 min), and the protein concentration was determined using protein assay reagent (Pierce, IL) according to the manufacturer's instructions. Quantified protein lysates (100 μg) were incubated for 4 h with 1 μg/ml anti-CLDN1 (Jay.8) or phospho-Ser/Thr PKA substrate antibodies at 4°C. Protein G-Sepharose beads (GE Healthcare, United Kingdom) were added, and following a 1-h incubation at 4°C, beads were collected by centrifugation and washed thoroughly in lysis buffer. Immunoprecipitated proteins were eluted from the protein G-Sepharose beads using Laemmli buffer, separated by 12% SDS-polyacrylamide gel electrophoresis (PAGE), and transferred onto polyvinylidene difluoride membranes (Sigma, United Kingdom) for incubation with anti-CLDN1 (Jay.8) or phospho-Ser/Thr PKA substrate antibodies (1 μg/ml). Secondary antibodies, HRP-conjugated donkey anti-rabbit and sheep anti-mouse IgG, were detected by enhanced chemiluminescence (Geneflow, United Kingdom).

Quantification of HCV RNA. To measure the effect of H89 treatment on intracellular and cell-free HCV RNA levels, RNA was extracted using the RNeasy mini kit (Qiagen, Germany) and a QIAamp MinElute virus kit (Qiagen, Germany), respectively, according to the manufacturer's instructions. The amplification efficiencies of cell-free HCV RNA preparations were assessed by the addition of a small quantity of exogenous HeLa RNA (10 pg) to the reverse transcription (RT)-PCR mixture. HCV amplification was performed using a modification of a method described previously by Cook and colleagues (25, 95) in a single-tube RT-PCR in accordance with the manufacturer's guidelines (CellsDirect kit; Invitrogen, CA), and fluorescence was monitored using a 7900 HT real-time PCR machine (ABI, CA) (71). In all reaction mixtures, the housekeeping gene glyceraldehyde-3-phosphate dehydrogenase (GAPDH) was included as an internal endogenous control for amplification efficiency and RNA quantification (primer-limited endogenous control; ABI).

Quantification of extracellular albumin, ApoB, and ApoE. Huh-7.5 cells were seeded at 6×10^4 cells/cm^2 in 48-well plates, subjected to a 3-h serum starvation the following day, and incubated with inhibitors diluted in serum-free DMEM for 1 h. Inhibitors were removed by washing, fresh 3% FBS–DMEM was added, and after 1 h the cell-free medium was collected and tested for levels of albumin (73), apolipoprotein B (ApoB), and apolipoprotein E (ApoE) using the following enzyme-linked immunosorbent assay (ELISA) protocols. Briefly, Immulon 2HB ELISA plates (Thermo, MA) were coated with goat anti-human albumin (Bethyl Laboratories, Montgomery, TX), and diluted samples or known standards were added for 1 h at room temperature. Bound albumin was detected with an HRP-conjugated goat anti-human albumin (Bethyl Laboratories, TX). ApoB and ApoE were measured using an in-house sandwich ELISA using rabbit anti-human ApoB or ApoE capture antibodies (Dako, Denmark). After blocking and washing, diluted samples or standards were added for 4 h at 37°C, and bound apolipoproteins were detected using HRP-conjugated rabbit anti-human ApoB or ApoE antibodies. Bound HRP conjugates were detected colorimetrically after reaction with a TMB substrate solution (BioFX, MD).

Quantification of HCV particle buoyant density. Linear iodixanol (Axis-Shield, United Kingdom) gradients were prepared using a two-chamber gradient maker (Jencons, United Kingdom) with light (6%) and dense (56%) iodixanol solutions (78). Gradients were used immediately after preparation, and 0.4 ml of virus was loaded onto each gradient. Samples were centrifuged at 100,000 $\times$ *g* for 21 h at 4°C in an L80-M ultracentrifuge (Beckman, United Kingdom). Fractions were harvested by tube puncture, and the density was determined using a digital refractometer (Atago, Japan). RNA was extracted from each fraction using a Qiamp viral RNA kit (Qiagen, Germany) and quantified for HCV RNA.

Quantification of intracellular cAMP levels. Naïve and HCV-infected cells (72 h postinfection) were seeded at 1.5×10^4 cells/cm^2, and cAMP levels were determined as an index of adenylate cyclase activity, as previously described (48). Cells were washed and incubated for 15 min at 37°C in medium containing 0.1% BSA and 0.5 mM IBMX. Cells were incubated for 1 h in the presence and absence of the cAMP agonist FK (10 μM), and reactions were terminated by washing in ice-cold PBS. Cytoplasmic contents were extracted by scraping cells into ice-cold 70% ethanol, and samples were stored on ice for 1 h. Supernatants were separated from cell debris by centrifugation, and the pelleted material was extracted with ethanol for 30 min and combined with the supernatants. Samples were dried under a vacuum, and cAMP levels were measured using the [^{3}H]cAMP Biotrak assay kit according to the manufacturer's instructions (GE Healthcare, United Kingdom).

RESULTS

Protein kinases and HCV entry. To study the involvement of protein kinases during HCVcc infection, we examined the effect of several inhibitors targeting PKC (Ro-31-8220), PKA (H89), MEK1 (PD98059), MEK1/2 (U0126), and p38 MAPK (SB203580) (20, 27, 33, 35, 56, 67). All inhibitors were used at a concentration that was nontoxic for Huh-7.5 cells in a 3-(4,5-dimethyl-2-yl)-5-(3-carboxymethoxyphenyl)-2-(4-sulfophenyl)-2H-tetrazolium assay (data not shown). Huh-7.5 cells were treated for 1 h with the various inhibitors and infected with JFH-1 for 1 h in the continued presence of the compounds. Treatment of cells with the PKA inhibitor H89 reduced JFH-1 infectivity by 80%, whereas PKC or MAPK inhibitors had no detectable effect (Fig. 1A). These results led us to study the role of PKA in HCV infection in more detail.

cAMP-dependent kinase (PKA) exists as an inactive holoenzyme complex comprising two regulatory (R) and two catalytic (C) subunits. Upon cAMP binding to the R subunits, the holoenzyme dissociates and releases the C subunits, which phosphorylate substrate proteins in the cytosol and nucleus. H89 competes with ATP binding to the C subunit(s) and prevents substrate phosphorylation (20). H89 treatment of Huh-7.5 cells led to a dose-dependent inhibition of J6/JFH and JFH-1 infectivity (Fig. 1B). However, H89 is reported to have off-target effects (65). To verify a role for the catalytic subunit of PKA (PKA-C) in HCV infection, we treated Huh-7.5 cells with a myristoylated version of the naturally occurring protein kinase inhibitor peptide (myrPKI) (44). myrPKI specifically inactivates PKA activity by binding to the C subunits with subnanomolar affinity (46, 54). The treatment of Huh-7.5 cells with myrPKI inhibits J6/JFH and JFH-1 infectivity in a dose-dependent manner (Fig. 1C), providing clear evidence for a role of PKA-C in HCV infection.

To assess whether PKA has a specific role in HCV entry, we studied the effect(s) of H89 and myrPKI on the ability of Huh-7.5 cells to support HCVpp infection. H89 inhibited HCVpp-JFH-1 infectivity in a dose-dependent manner and had no effect on MLVpp infectivity (Fig. 2A), confirming a specific inhibition of particles bearing HCV GPs. myrPKI demonstrated a dose-dependent inhibition of HCVpp-H77 entry and no detectable effect(s) on MLVpp infectivity (Fig. 2B), further validating a role for PKA in HCV entry. To ascertain whether the inhibitory effect of H89 was apparent in other cell types, a range of cells were incubated with H89 as previously

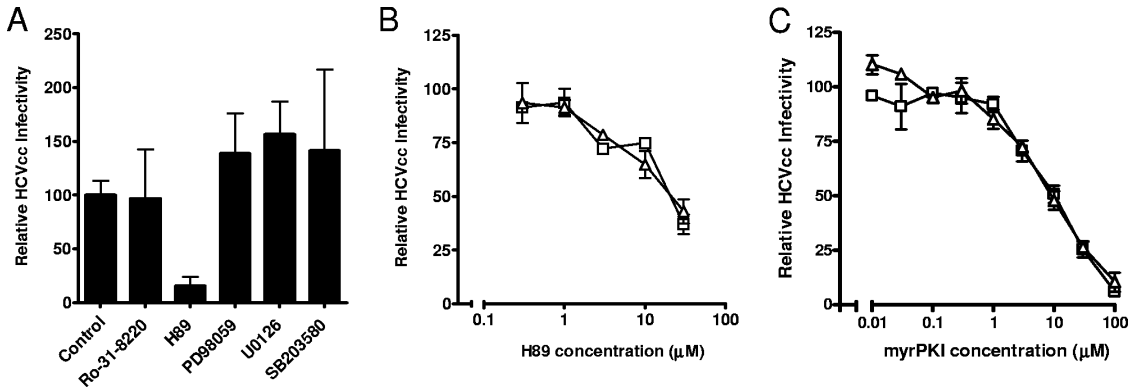

FIG. 1. Inhibition of PKA attenuates HCV infection. (A) Huh-7.5 cells were incubated with Ro-31-8220 (1 μM) (PKC inhibitor), H89 (10 μM) (PKA inhibitor), PD98059 (10 μM) (MEK1 inhibitor), U0126 (10 μM) (MEK1/2 inhibitor), or SB203580 (10 μM) (p38MEK inhibitor) for 1 h and infected with JFH-1 for 1 h in the presence of inhibitors. (B) Dose-dependent reduction of HCV infection by H89 inhibition of PKA. Huh-7.5 cells were incubated for 1 h with increasing concentrations of H89 and infected with J6/JFH (□) or JFH-1 (△). (C) Dose-dependent reduction of HCV infection by myrPKI inhibition of PKA. Huh-7.5 cells were incubated for 1 h with increasing concentrations of myrPKI and infected with J6/JFH (□) or JFH-1 (△). Infectivity is expressed relative to untreated control cells and represents the mean of three replicate infections. The data presented are from a single experiment and are representative of three independent experiments.

described. H89 inhibited HCVpp infection of all cell types tested, including primary human hepatocytes (Fig. 2C), with no discernible effect on MLVpp infectivity (data not shown). Since HCVpp allow us to study GP-dependent entry independent of downstream replication and translation events, we can conclude that PKA has a role in HCV entry.

Inhibition of PKA can also be achieved by cAMP antagonists, which bind to the R subunit(s) and prevent holoenzyme dissociation and activation. PKA exists as two isoforms defined by their respective regulatory subunits, types I and II. Rp-8-Br-cAMPS has been reported to preferentially inhibit PKAI (30, 39, 66), whereas Rp-cAMPS inhibits both isoforms. To discriminate a role for PKAI and PKAII, we studied the effect of Rp-8-Br-cAMPS and Rp-cAMPS on the ability of Huh-7.5 cells to support HCV infection. Rp-cAMPS reduced J6/JFH and JFH-1 infectivity, whereas Rp-8-Br-cAMPS had no effect (Fig. 3A), suggesting a role for PKAII in HCV infection. To ascertain whether the cAMP antagonists have differential effects on PKAI and PKAII in Huh-7.5 cells, we used BRET to study the PKA subunit interaction(s) with isoform-specific PKA sensors. R and C subunits of PKA were tagged with Rluc as a bioluminescent donor or GFP as a fluorescent acceptor, respectively, allowing the quantitative comparison of PKAI and PKAII regulation (83). Following PKA activation, the holoenzyme dissociates, leading to a reduced BRET signal. FK activates PKA by stimulating cAMP levels, causing the phosphorylation of substrates including phosphodiesterases (PDEs), which degrade cAMP and thereby reduce PKA activity.

To assess the antagonistic effect(s) of the Rp analogs on PKAI and PKAII isoforms, we measured their ability to inhibit FK/IBMX-induced holoenzyme dissociation. IBMX is a general PDE inhibitor and is a prerequisite to observe effects on the PKAI BRET sensor (83). In the presence of FK and IBMX, Rp-8-Br-cAMPS and, to a lesser extent, Rp-cAMPS could inhibit the type I BRET sensor but not the type II sensor (Fig. 3B), suggesting specificity of Rp-8-Br-cAMPS for PKAI. This effect is probably due to the differential distribution of PKAI versus PKAII, where PKAII is clustered in subcellular compartments via AKAPs to the plasma membrane and can be stimulated by FK alone (96). Thus, the FK activation of PKA in the presence of PDE inhibitors prolongs the time period of PKA activity. In contrast, FK treatment failed to activate the PKAI BRET sensor (Fig. 3C). However, PKAII dissociation was promoted by endogenously elevated cAMP levels in response to FK alone; this effect was reversed with Rp-cAMPS but not Rp-8-Br-cAMPS, indicating PKA type II involvement (Fig. 3C).

To investigate whether stimulating PKA activity enhances HCV entry, Huh-7.5 cells were treated with FK for 1 h and tested for their ability to support HCVcc and HCVpp infection. FK treatment increased J6/JFH and JFH-1 infectivity by 72% and 165%, respectively (Fig. 4A). This increase in infectivity could be abrogated by prior treatment of cells with H89 (10 μM) (Fig. 4A), confirming the PKA dependency of the effect. In contrast, FK treatment had no effect on HCVpp-JFH-1 infectivity (Fig. 4B), suggesting that FK promotes HCV infection postentry. No significant differences in the effect(s) of FK treatment on HCV infection in the presence or absence of IBMX were noted (data not shown).

Inhibition of PKA activity induces a reorganization of CLDN1 in Huh-7.5 cells. HCV utilizes the cellular molecules CD81, SR-BI, and CLDN1 to enter target cells. To investigate whether the inhibitory activity of H89 involves these receptor molecules, we studied their expression and localization in control or H89- or FK-treated cells. Flow cytometry demonstrated that CD81, SR-BI, and CLDN1 expression levels were not altered by H89 treatment (data not shown). H89 induced an altered staining pattern of CLDN1, whereas CD81 localization was unchanged (Fig. 5A). In untreated cells, CLDN1 localized to the plasma membrane, predominantly at intercellular junctions, whereas a fragmented pattern of plasma membrane staining with intracellular CLDN1 was observed in H89-treated cells (Fig. 5A). FK treatment had no detectable effect on CLDN1 or CD81 localization. Rp-cAMPS induced a pattern of CLDN1 localization similar to that seen with H89 (Fig. 5A), whereas the Rp-8-Br-cAMPS had no effect (Fig. 5A).

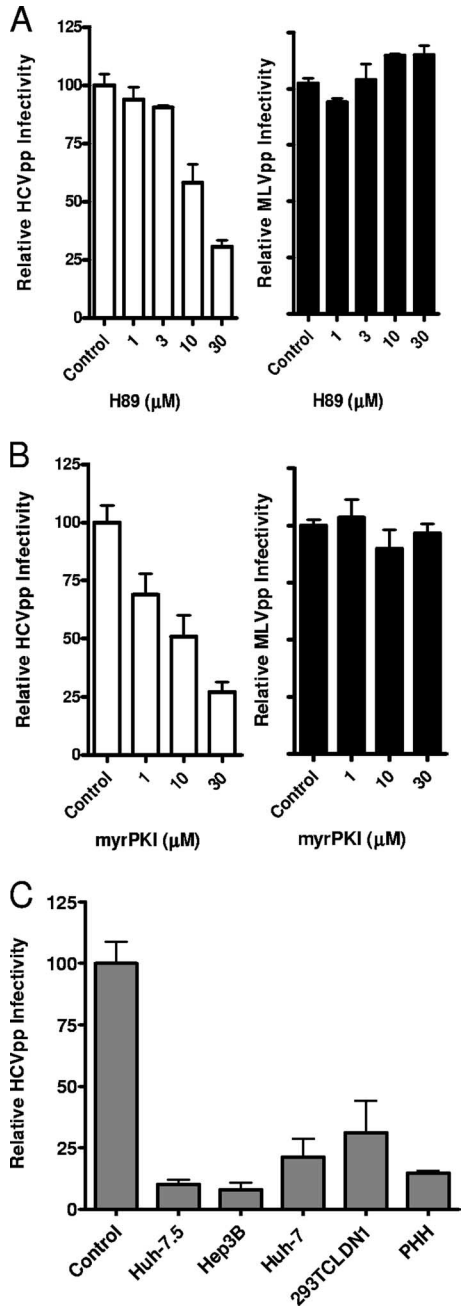

FIG. 2. PKA-dependent HCV entry. (A) Dose-dependent reduction of HCVpp entry by H89 inhibition of PKA. Huh-7.5 cells were incubated for 1 h with increasing concentrations of H89 and infected with HCVpp-JFH-1 (white bars) or MLVpp (black bars). (B) Dose-dependent reduction of HCVpp entry by myrPKI inhibition of PKA. Huh-7.5 cells were incubated for 1 h with increasing concentrations of myrPKI and infected with HCVpp-H77 (white bars) or MLVpp (black bars). (C) Huh-7.5, Hep3B, Huh-7, 293T-CLDN1, and primary human hepatocytes (PHH) were incubated with H89 (10 μM) for 1 h and infected with HCVpp-H77. HCVpp-JFH-1 infection was assessed by flow cytometry, while for HCVpp-H77 infection, the cells were lysed, and the mean luciferase activity (relative light units) was measured; for all samples, the average Env^-pp value was subtracted. Infectivity is expressed relative to those of untreated control cells and represents the mean of data from three replicate infections. The data presented are from a single experiment and are representative of three independent experiments.

Neither of the PKA-specific inhibitors had an effect on CD81 localization. Attempts to visualize SR-BI in control or treated cells with monoclonal and polyclonal antibodies specific for SR-BI were unsuccessful, probably reflecting the low level of SR-BI expression in Huh-7.5 cells. To investigate whether inhibiting PKA altered the localization of other TJ proteins, control and H89-treated cells were stained for zonula occludens type 1 (ZO-1) and occludin expression. H89 had no effect on ZO-1 or occludin localization in Huh-7.5 cells (Fig. 5B).

PKA can be targeted to sites of potential substrates by AKAPs, allowing the coordination of multiple signal transduction pathways. AKAP-IS is a potent and selective antagonist of PKAII (1, 100, 101). Huh-7.5 cells were transfected to express GFP-tagged AKAP-IS or a scrambled control peptide, and CLDN1 localization was assessed. Typical plasma membrane localization of CLDN1 was observed in cells expressing the scrambled peptide; however, CLDN1 demonstrated an intracellular localization in AKAP-IS-expressing cells (Fig. 5C). CD81 expression and localization were unaltered in AKAP-IS- or scrambled control peptide-expressing cells (data not shown). These data lend further support for a role of PKAII in CLDN1 localization and HCV entry.

Imaging techniques that take advantage of FRET between fluorescent proteins have been developed to study their association. We recently demonstrated FRET between DsRed-CLDN1 (r.CLDN1) and AcGFP-CD81 (g.CD81) at the plasma membrane, consistent with a subpopulation of molecules forming a coreceptor complex (43). To elucidate a role of PKA in the CLDN1 association with CD81, Huh-7.5 cells expressing g.CD81 (donor) and r.CLDN1 (acceptor) were treated with H89 or FK, and the frequency of proteins in close enough proximity (<10 nm) for FRET to occur was assessed (percent FRET). H89 significantly reduced the frequency of FRET between CD81 and CLDN1 (FRET of 50.0% for control cells and 20.8% for H89-treated cells [$P < 0.05$ by Fisher's exact test]), whereas FK treatment had no significant effect (35.0% [not significant]). These data suggest that the PKA-dependent localization of CLDN1 at the plasma membrane is important for CLDN1 association with CD81.

PKA-dependent infectivity of extracellular HCV. In hepatocytes, cAMP/PKA activity was previously reported to be important for the trafficking of lipids and apical plasma membrane proteins (97, 100, 102, 106). We were interested to determine whether PKA has a role in the secretion and infectivity of extracellular HCV. J6/JFH- and JFH-1-infected cells (>80% $NS5A^+$) were treated with increasing concentrations of H89 for 1 h, the cells were washed extensively to remove inhibitor, and the amount of infectious virus released from control or treated cells was assessed. J6/JFH- and JFH-1-infected Huh-7.5 cells released 1.7×10^4 and 6.8×10^4 IU/ml, respectively. H89 treatment reduced the titer of infectious extracellular virus, with the highest dose (30 μM) reducing the infectivities of J6/JFH and JFH-1 by 90% and 75%, respectively (Fig. 6A). In contrast, H89 had no effect on the infectivity of intracellular virus (Fig. 6B). The effects of H89 were previously reported to be reversible (13), and we found that an 8-h "recovery period" following H89 treatment was sufficient to restore extracellular virus infectivity to levels observed in the untreated cultures (data not shown). Incubation of Huh-7.5 cells with myrPKI induced a dose-dependent decrease in ex-

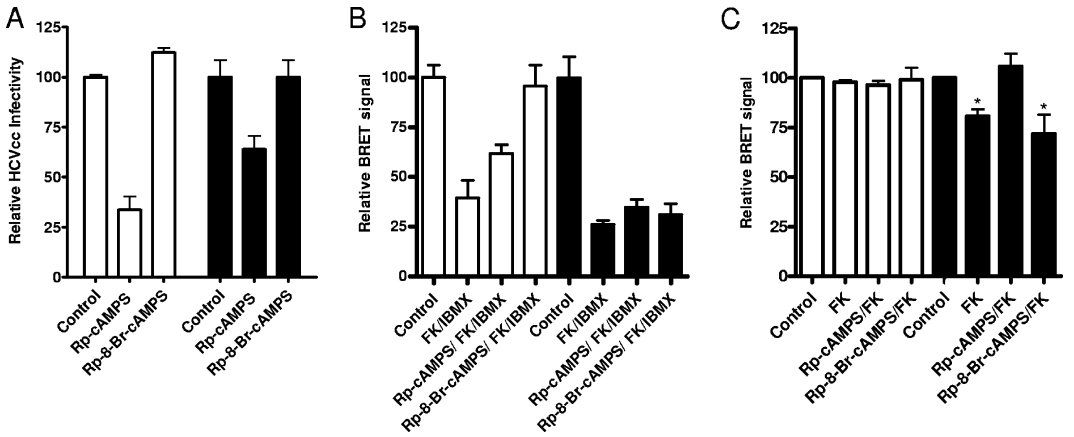

FIG. 3. Putative role for PKAII in HCV infection. (A) Huh-7.5 cells were incubated with the cAMP analogs Rp-cAMPS (500 μM) or Rp-8-Br-cAMPS (500 μM) and infected for 1 h with J6/JFH (white bars) or JFH-1 (black bars). HCVcc-infected cells were fixed after 48 h and stained for NS5A, and the mean number of infected cells per well was determined by flow cytometry. Infectivity is expressed relative to untreated control cells and represents the mean of data from three replicate infections. The data presented are from a single experiment and are representative of three independent experiments. (B) Huh-7.5 cells expressing PKAIα (white bars) or PKAIIα (black bars) sensors were preincubated with Rp-cAMPS (500 μM) or Rp-8-Br-cAMPS (500 μM) for 1 h, followed by FK/IBMX (50 μM and 500 μM, respectively) stimulation for 30 min. The BRET signal was quantified using a Fusionα FP microplate reader, and data are plotted relative to untreated control cells. The data were compiled from three independent experiments. (C) Huh-7.5 cells expressing PKAIα (white bars) or PKAIIα (black bars) sensors were preincubated with Rp-cAMPS (500 μM) or Rp-8-Br-cAMPS (500 μM) for 1 h, followed by FK (10 μM) stimulation for 30 min. The data presented are compiled from three independent experiments. Statistical analysis using a Newman-Keuls multiple-comparison test confirms that FK treatment significantly reduced the BRET signal compared to those of control untreated cells ($P < 0.05$), while pretreatment with Rp-cAMPS had no significant effect on the BRET signal relative to the control. Preincubation of cells with Rp-8-Br-cAMPS did not inhibit the FK-stimulated decrease in BRET signal compared to the control.

tracellular J6/JFH and JFH-1 virus infectivity by 62% and 80%, respectively, at the highest dose (100 μM), confirming a specific role for PKA.

To further corroborate PKA specificity and to determine which isoform modulates virus infectivity, infected cells were incubated for 1 h with Rp-cAMPS or Rp-8-Br-cAMPS, and cell-free virus infectivity was measured. Rp-cAMPS inhibited the level of infectious JFH-1 and J6/JFH cell-free virus, whereas Rp-8-Br-cAMPS did not, suggesting that PKAII modulates extracellular virus infectivity (Fig. 6D). To investigate whether FK stimulation of PKA modulates the infectivity of cell-free virus, infected cells were incubated with FK (10 μM) for 1 h, the inhibitor was removed, and the infectivity of cell-free virus was assessed. FK treatment increased the level of infectious J6/JFH and JFH-1 cell-free virus, and this effect could be inhibited by H89 (10 μM), demonstrating PKA dependency (Fig. 6E).

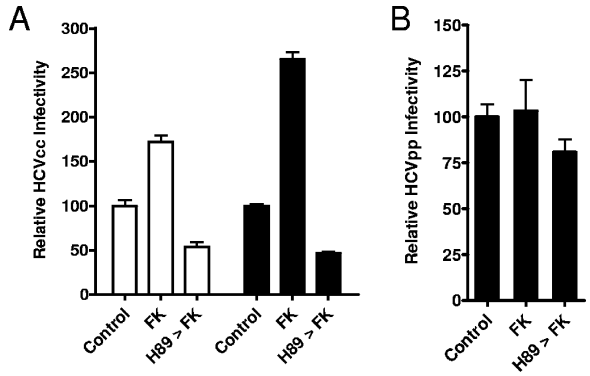

FIG. 4. FK activation of PKA enhances HCV infection. Huh-7.5 cells were incubated with FK (10 μM) (PKA activator) for 1 h with or without a 1-h preincubation with H89 (10 μM) (PKA inhibitor). Cells were infected with J6/JFH (white bars) or JFH-1 (black bars) (A) and HCVpp-JFH (B) for 1 h in the presence of PKA modulators. HCVcc-infected cells were fixed after 48 h and stained for NS5A, and the mean number of infected cells per well was determined by flow cytometry. For HCVpp, the cells were lysed, the mean luciferase activity (relative light units) was measured, and the average Env^-pp value was subtracted. Infectivity is expressed relative to untreated control cells and represents the mean of data for three replicate infections. The data presented are from a single experiment and are representative of three independent experiments.

To determine whether H89 affects the release of virus particles or their infectivity, we measured viral RNA in the cell-free medium from control and treated cells (25, 28). The treatment of infected cells with H89 for 1 h or 24 h had no significant effect on the levels of cell-free viral RNA secreted from cells or on the intracellular levels of HCV RNA (Fig. 7A and B). Since the cAMP/PKA pathway has been implicated in the regulation of exocytosis in secretory cells (69, 90, 102), we investigated whether H89 treatment modulates Huh-7.5 secretion of albumin. The level(s) of albumin released from naïve or HCV-infected cells was similar and not altered by H89 or FK treatments (Fig. 7C), suggesting that the general secretory pathway was not affected. These data demonstrate that inhibiting PKA activity decreases the infectivity of extracellular virus without inhibiting viral RNA replication or virus particle release, suggesting a PKA-dependent step in the infectivity or maturation of HCV particles.

Stability of extracellular HCV infectivity. We noted that extracellular J6/JFH and JFH-1 infectivity declined over time at 37°C (Fig. 8A); this loss in infectivity was not associated with a decline in HCV RNA levels (Fig. 8B). To investigate whether

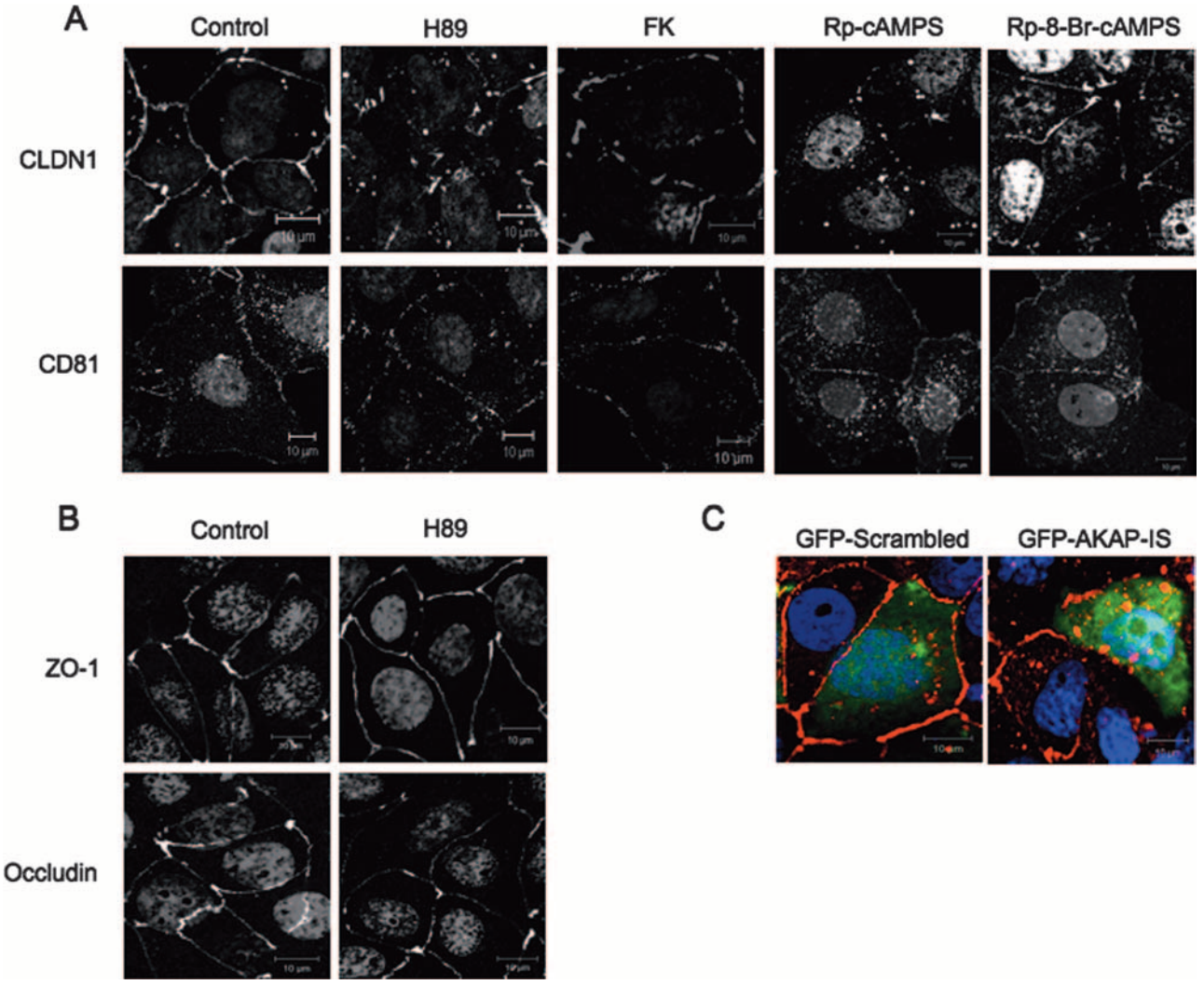

FIG. 5. Inhibition of PKA disrupts CLDN1 localization in Huh-7.5 cells. (A) Huh-7.5 cells were seeded onto glass coverslips and incubated with dimethyl sulfoxide (DMSO) (control), H89 (10 μM), FK (10 μM), Rp-cAMPS (500 μM), or Rp-8-Br-cAMPS (500 μM). Cells were fixed and stained for CLDN1 or CD81. (B) Huh-7.5 cells were incubated with DMSO (control) or H89 (10 μM) for 1 h, fixed, and stained for the TJ proteins ZO-1 and occludin. Bound antibodies were visualized using Alexa Fluor 488 anti-mouse Ig. (C) Huh-7.5 cells were transduced to express GFP-AKAP-IS or GFP-Scrambled peptide (green) and stained for CLDN1. Bound antibodies were visualized using Alexa Fluor 633 anti-mouse antibodies (red). Nuclei were visualized using DAPI (blue). Laser scanning confocal microscopic images of single 1-μm *z* sections were obtained using a 63× 1.2-numerical-aperture objective (scale bar represents 10 μm).

PKA modulates the stability of extracellular virus infectivity, JFH-1-infected cells were treated with H89 for 1 h, and the extracellular virus was harvested during the first hour following H89 removal and incubated at 37°C for 1 and 8 h. Virus released from control or H89-treated cells showed a similar loss of infectivity at 37°C over time, suggesting that PKA does not alter or modulate the temperature-dependent properties of extracellular virus infectivity (Fig. 8C).

Role of PKA in ApoB and ApoE secretion and buoyant density of cell-free HCV particles. HCV replicates in cytoplasmic membrane vesicles, which are enriched with ApoB, ApoE, and microsomal triglyceride transfer protein (MTP), proteins known to be required for the assembly of very-low-density lipoprotein (VLDL) (50). Recent reports demonstrated that the treatment of hepatoma cells with an MTP inhibitor and small interfering RNA silencing of ApoB and ApoE expression reduced the levels of VLDL and HCV in the extracellular medium, suggesting that viral secretion is dependent on VLDL assembly and/or release (19, 38, 50). To ascertain whether H89 treatment of Huh-7.5 cells alters lipoprotein secretion, we quantified ApoB and ApoE levels released from control and treated cells. H89 reduced ApoB secretion from naïve (data not shown) and HCV-infected cells but had a negligible effect on ApoE levels (Fig. 9A).

Extracellular HCVcc particles have been reported to have a heterogeneous range of buoyant densities, with the lower-density forms representing VLDL-associated particles (38, 64, 78). To assess whether the effects of H89 on ApoB secretion and viral infectivity reflect an altered association of particles with lipoproteins and the concomitant change in particle buoyant density, we utilized iodixanol gradients to determine the buoyant density of cell-free virus (63, 64, 78). Virus-containing

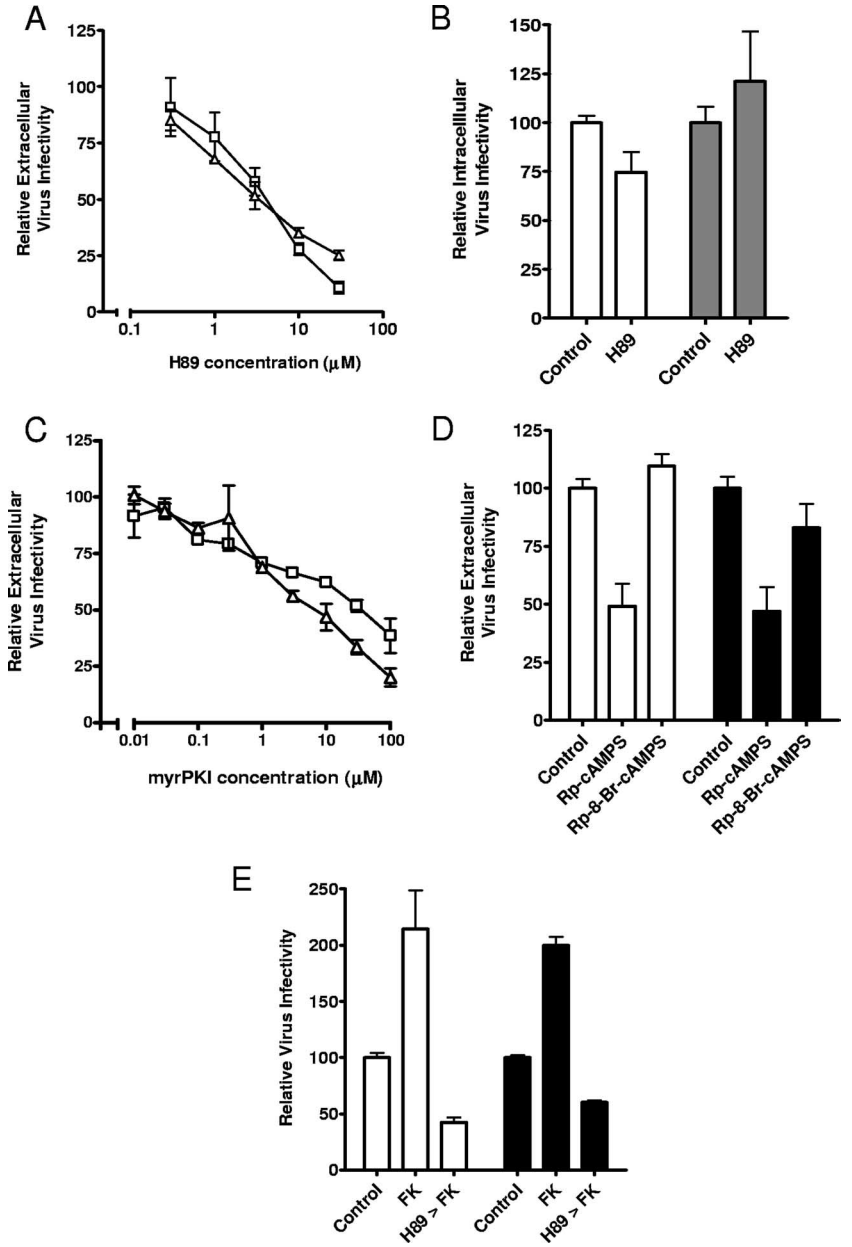

FIG. 6. PKA-dependent infectivity of extracellular HCV. (A) Dose-dependent reduction in extracellular HCV infectivity by H89. J6/JFH (□)- and JFH-1 (△)-infected Huh-7.5 cells were seeded in 48-well plates and incubated with increasing concentrations of H89 the following day. Cells were extensively washed, supernatant was collected after 1 h, and infectivity was quantified. (B) J6/JFH-infected cells were incubated with H89 (10 μM) for 1 h (white bars) or 8 h (gray bars), the intracellular virus was released by repeated freeze-thaw cycles, and infectivity was quantified. (C) Dose-dependent reduction in extracellular HCV infectivity by myrPKI. J6/JFH (□)- and JFH-1 (△)-infected Huh-7.5 cells were seeded in 48-well plates and incubated with increasing concentrations of myrPKI the following day. Cells were extensively washed, supernatant was collected after 1 h, and infectivity was quantified. (D) The infectivity of extracellular virus obtained from J6/JFH (white bars)- and JFH-1 (black bars)-infected Huh-7.5 cells incubated with the isoform-specific PKA inhibitors Rp-cAMPS (500 μM) or Rp-8-Br-cAMPS (500 μM) for 1 h was measured. (E) The infectivity of extracellular virus from J6/JFH (white bars)- and JFH-1 (black bars)-infected Huh-7.5 cells incubated for 1 h with FK (10 μM) (PKA activator) in the presence and absence of H89 pretreatment (10 μM). Virus infectivity was determined by infection of naïve Huh-7.5 cells, and NS5A-positive cells were enumerated. Infectivity is expressed relative to control untreated cells and represents the mean of three replicate infections. The data presented are from a single experiment and are representative of three independent experiments.

supernatant from control and H89-treated cells was analyzed on an iodixanol gradient, and the density of HCV RNA-containing fractions was determined. The distributions of particle densities from control (Fig. 9B) or H89-treated cells (Fig. 9C) were comparable. HCV exhibited a bimodal distribution of buoyant density with peaks of HCV RNA at 1.155 and 1.087 g/ml for the control and at 1.152 and 1.086 g/ml for virus from H89-treated cells. This is consistent with data from previous reports (63, 64, 78) and suggests that the reduced infectivity is not due to an altered particle buoyant density.

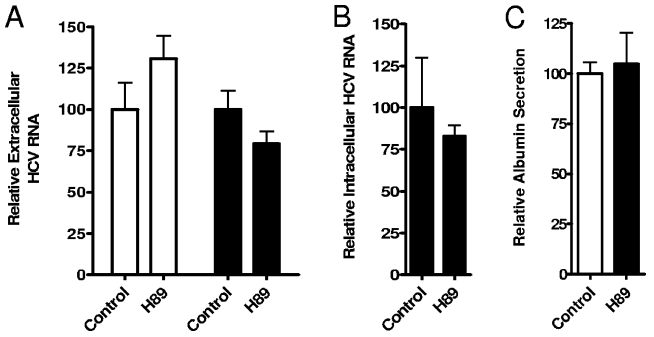

FIG. 7. Inhibition of PKA does not affect extracellular or intracellular HCV RNA. Extracellular (A) and intracellular (B) HCV RNA levels were quantified in control and H89 (10 μM)-treated JFH-1-infected Huh-7.5 cells. Cells were incubated with H89 for 1 h (white bars) or 24 h (black bars). HCV RNA was detected by RT-PCR and quantified relative to a GAPDH control. (C) Effect of H89 on Huh-7.5 secretion of albumin. Huh-7.5 cells were treated with a DMSO control or H89 (10 μM) for 1 h, and the levels of albumin in the extracellular medium were quantified by ELISA. Data are expressed relative to those for control untreated cells and represent values from the means of three replicate infections. The data presented are from a single experiment and are representative of two independent experiments.

HCV infection promotes cAMP levels and PKA activity. Given the effects of H89 and FK on HCV entry and extracellular virus infectivity, we were interested to investigate whether infection modulates cAMP levels and PKA activity. Increased cAMP levels were detected in J6/JFH- and JFH-1-infected Huh-7.5 cells 72 h postinfection (>80% $NS5A^+$) compared to naïve cells (Fig. 10A). As a control, naïve Huh-7.5 cells were shown to be highly responsive to FK treatment, demonstrating a 78-fold increase in cAMP levels (Fig. 10A). Incubation of Huh-7.5 cells with HCVcc virus or E1E2 glycoproteins for 1 h had no detectable effect on cAMP levels (data not shown).

To assess whether the elevated cAMP levels observed in HCV-infected cells activates PKA, we measured the reactivity of an antibody specific for the phosphorylated PKA substrate consensus motif (p-PKAs) with protein lysates from naïve and HCV-infected cells 72 h following infection (17, 61, 79). As

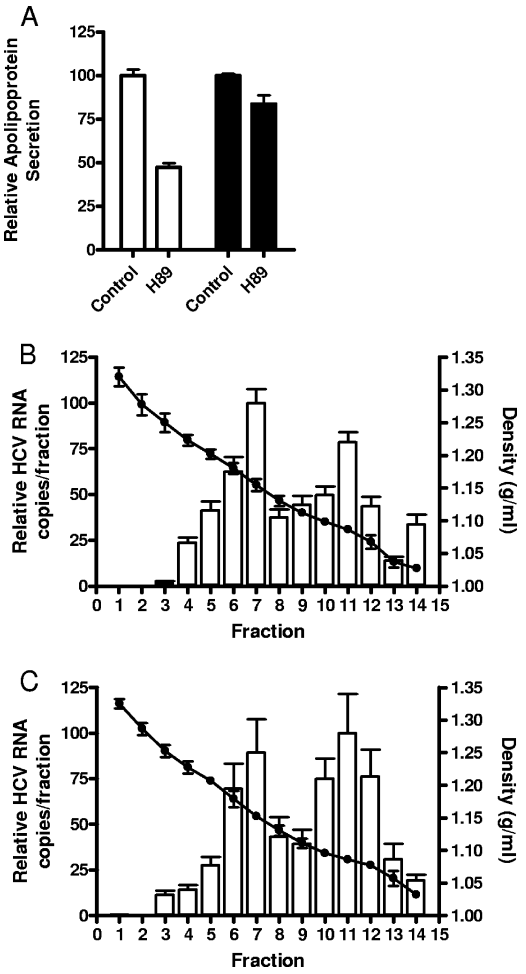

FIG. 9. Effects of PKA modulators on ApoB and ApoE secretion and HCV particle buoyant density. (A) Extracellular medium was collected from control and H89 (10 μM)-treated Huh-7.5 cells, and the levels of ApoB (white bars) and ApoE (black bars) were measured by capture ELISA. Data are expressed relative to those for control untreated cells and represent the mean of data for three replicate infections. The buoyant density (●) of extracellular J6/JFH released from control (B) or H89-treated (C) Huh-7.5 cells was determined on iodixanol gradients. Individual bars show relative HCV RNA copy numbers in each fraction compared to the maximum peak.

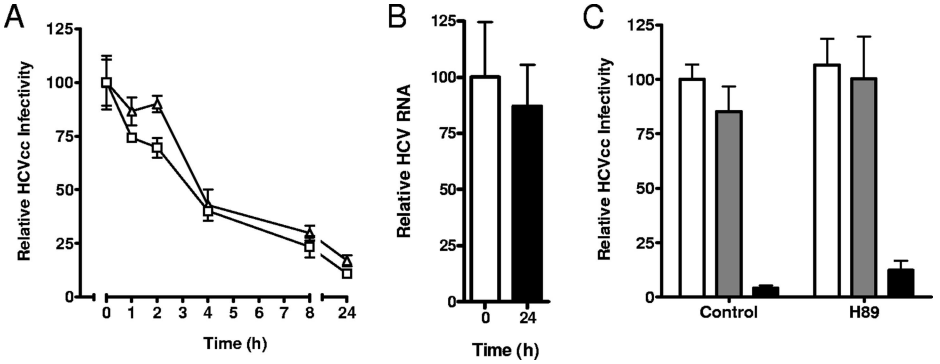

FIG. 8. PKA does not regulate the stability of infectious extracellular virus. (A) The infectivities of extracellular J6/JFH (□) and JFH-1 (△) were assessed after incubation of the virus at 37°C for 0, 1, 2, 4, 8, and 24 h. (B) The HCV RNA content of extracellular J6/JFH was measured preincubation (white bars) and postincubation (black bars) of virus at 37°C for 24 h. HCV RNA was detected by RT-PCR and quantified relative to a GAPDH control. (C) Effect of H89 on the stability of extracellular JFH-1 infectivity. Extracellular virus was collected from control and H89 (10 μM)-treated JFH-1-infected Huh-7.5 cells and incubated at 37°C for 0 h (white bars), 1 h (gray bars), or 8 h (black bars), and infectivity was assessed. Data are expressed as relative infectivity compared to control untreated cells and represent the means of data from three replicate infections. The data presented are from a single experiment and are representative of two independent experiments.

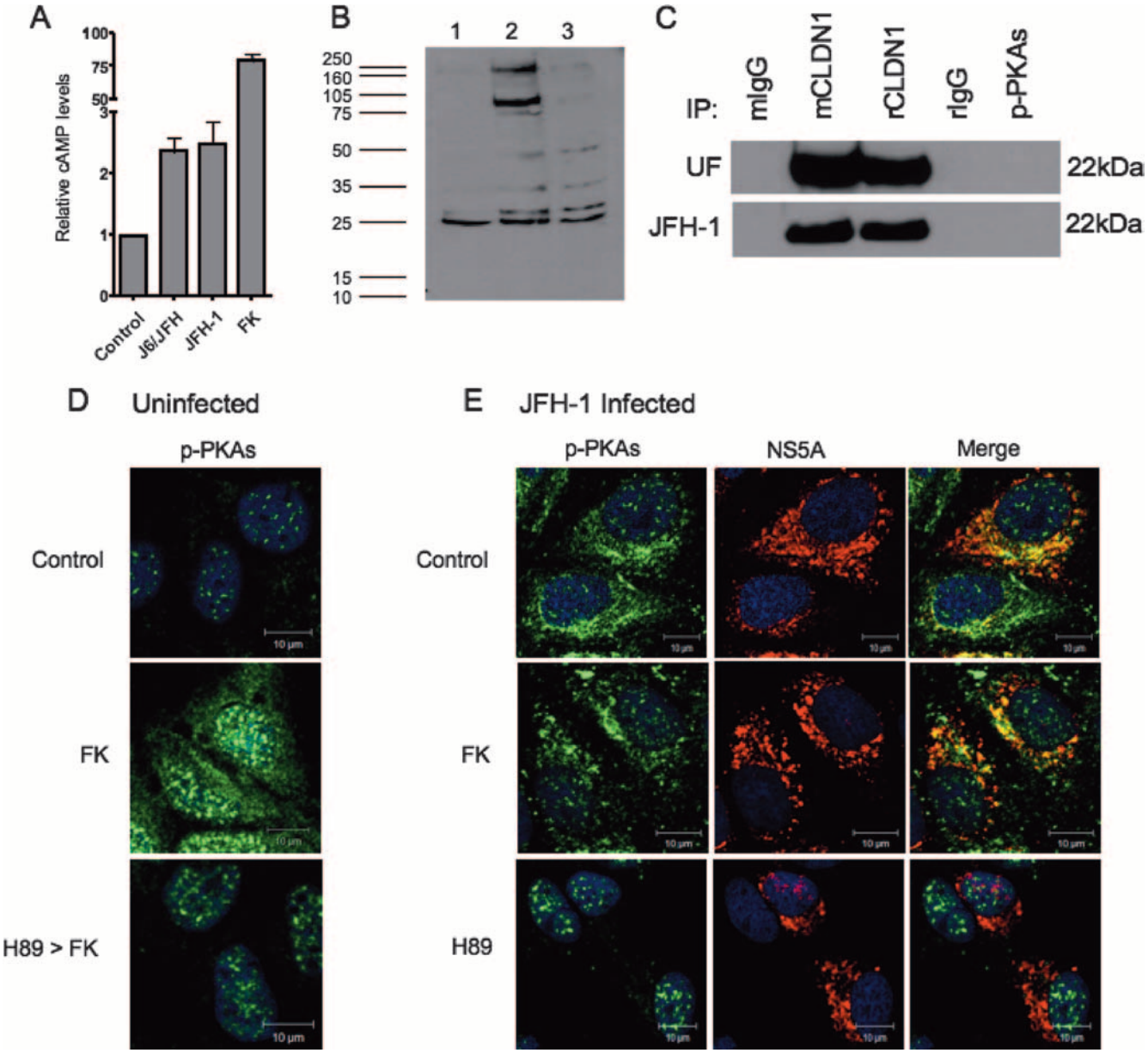

FIG. 10. HCV infection increases cAMP levels and PKA activity. (A) cAMP levels were measured in uninfected and J6/JFH- and JFH-1-infected Huh-7.5 cells 72 h postinfection. As a control, Huh-7.5 cells were incubated with FK (10 μM), a compound known to activate adenylyl cyclase and increase cAMP levels. cAMP levels are shown relative to control untreated cells and represent data from the means of three replicate wells. (B) PKA activity was assessed by measuring the reactivity of an anti-PKA substrate-specific antibody (p-PKAs) with 10 μg of total protein separated by SDS-PAGE from control (lane 1), FK (10 μM)-stimulated (lane 2), and JFH-1-infected (72 h postinfection) (lane 3) Huh-7.5 cells. (C) CLDN1 and PKA substrates were immunoprecipitated from 100 μg of uninfected (UF) and JFH-1-infected (72 h postinfection) Huh-7.5 cell lysates with specific antibodies (mouse anti-CLDN1, rabbit anti-CLDN1, and p-PKAs) and control antibodies (murine IgG [mIgG] and rabbit Ig [rIgG]). Immunoprecipitates were subjected to SDS-PAGE, and reactivity with rabbit anti-CLDN1 was assessed by Western blotting. (D and E) Uninfected (D) and JFH-1-infected (E) (72 h postinfection) Huh-7.5 cells were incubated with FK or H89 for 1 h (H89 > FK indicates a 1-h preincubation with H89 prior to FK treatment), fixed, and stained with the PKA substrate-specific antibody (p-PKAs) (green). JFH-1-infected cells were visualized by staining for NS5A (red), and nuclei were counterstained with DAPI (blue). Laser scanning confocal microscopic images of single 1-μm *z* sections were obtained using a 63× 1.2-numerical-aperture objective (scale bar represents 10 μm).

expected, FK stimulation led to an increase in the number and intensity of bands representing phosphorylated PKA substrates compared to those of untreated cells (Fig. 10B). JFH-1 infection also increased the intensity and number of phosphorylated PKA substrates compared to those of uninfected cells (Fig. 10B). The molecular masses of PKA substrates observed in FK-treated and JFH-1-infected Huh-7.5 cells were comparable; however, a 22-kDa band corresponding to the molecular mass of CLDN1 was not detectable. To investigate whether CLDN1 is a direct substrate for PKA, CLDN1 and PKA substrates were immunoprecipitated from naïve and JFH-1-infected Huh-7.5 cell lysates, and the proteins were separated by

SDS-PAGE and tested for reactivity with antibodies specific for CLDN1 and PKA substrate. Anti-CLDN1 antibodies readily precipitated CLDN1 from cell lysates; however, these proteins were not recognized by p-PKAs (Fig. 10C). We observed no evidence of CLDN1 phosphorylation by PKA in Huh-7.5 cells incubated for 1 h with either HCVcc or E1E2 (data not shown).

To study PKA activity at the cellular level, naïve and JFH-1-infected Huh-7.5 cells were incubated with FK (10 μM) or H89 (10 μM) for 1 h, fixed, and stained with p-PKAs and NS5A-specific Abs. FK-treated naïve cells demonstrated increased cytoplasmic staining with p-PKAs that was abrogated by prior treatment with H89, indicating a cytoplasmic localization of PKA substrates (Fig. 10D). JFH-1-infected cells displayed increased cytoplasmic staining with p-PKAs compared to uninfected cells, which was abrogated by treatment with H89 (Fig. 10E), while FK did not increase p-PKA cytoplasmic staining in infected cells. The intracellular PKA substrate staining did not colocalize with anti-CLDN1 (data not shown), further suggesting that CLDN1 is not a direct substrate for PKA. In summary, these data show that HCV infection of Huh-7.5 cells leads to an increase in cAMP levels, which in turn activates PKA to phosphorylate various cellular targets, which may promote the infectivity of extracellular virus and increase viral transmission within the culture.

DISCUSSION

Protein kinases have been implicated in the life cycle of many viruses including adenovirus, herpes simplex virus, and influenza virus (91, 93, 103). By screening a series of kinase inhibitors for their effect(s) on HCV infection, we identified PKA as having an important role both in HCV entry and in the genesis of infectious extracellular virus.

Treatment of Huh-7.5 cells with the general PKA-C inhibitor H89, the specific PKA-C inhibitor myrPKI, and cAMP antagonist Rp-cAMPS inhibited HCVcc and HCVpp infection (Fig. 1 to 3), demonstrating that HCV internalization is dependent on the target cell expression of active PKA. A similar level of inhibition of HCVpp entry was noted for other cell types, including primary human hepatocytes, demonstrating the generality of this observation. Since HCV entry is dependent on the host cell expression of CD81, SR-BI, and CLDN1, we investigated whether inhibition of PKA altered viral receptor expression and localization. H89 or Rp-cAMPS had no effect on total coreceptor expression levels when quantified by flow cytometry or Western blotting. However, confocal imaging of treated cells identified intracellular forms of CLDN1 with reduced levels of expression at the plasma membrane (Fig. 5A). CD81 localization was unchanged in H89-, Rp-cAMPS-, or FK-treated cells (Fig. 5A). There was no discernible effect of FK treatment on CLDN1 localization (Fig. 5A), consistent with the negligible effect on HCVpp infection. These data support a model where CLDN1 localization at the plasma membrane is dependent on PKA and is essential for viral receptor activity.

We (43) and others (104) previously reported that CLDN1 associates with CD81 at the plasma membrane of Huh-7 cells, suggesting that coreceptor complexes have a role to play in the viral entry process. The observation that H89 treatment reduced FRET between CLDN1 and CD81 lends further support for a PKA-dependent localization of CLDN1 at the plasma membrane.

The cellular localization of several members of the CLDN family is reported to be regulated by growth factors (92) and kinases: CLDN1 by MAPK (37), CLDN3 by PKA (31), CLDN4 by EphA2 (94) and PKC (32), and CLDN16 by PKA (51). The functional consequences of CLDN phosphorylation are specific for certain CLDN family members and are most likely dependent upon the cell type under study. CLDN1 contains several potential PKA phosphorylation sites located at amino acids S34 and S69 in the first extracellular loop, S173 in the first transmembrane domain, and T190 in the C-terminal cytoplasmic region. Evans and colleagues previously reported that amino acids I32 and E48 within extracellular loop 1 of CLDN1 are critical for coreceptor activity (34), with I32 forming part of the PKA phosphorylation consensus site. During the dynamic remodeling of tight junctions, claudins have been reported to internalize (70); indeed, we have observed intracellular forms of CLDN1 in Huh-7.5 cells (M. J. Farquhar, unpublished observations). Consequently, it is feasible that residues within the extracellular loops may be targets for PKA phosphorylation. The entire C-terminal CLDN1 tail is not required for HCV coreceptor activity in 293T embryonal kidney cells (34, 43), suggesting that this region is not the site for PKA phosphorylation. This is in contrast to recent reports demonstrating the importance of CLDN3 and CLDN16 C-terminal cytoplasmic tails in PKA phosphorylation (31, 51). However, we were unable to demonstrate CLDN1 recognition by a PKA substrate-specific antibody (Fig. 10B and C), suggesting that CLDN1 is not directly phosphorylated by PKA. It should be noted that CLDN1 is an integral membrane protein that associates with other intercellular junctional and associated cytosolic proteins that may be modulated by PKA (5, 57, 58).

PKA plays an important role in the regulation of protein trafficking along the constitutive secretory pathway and has been implicated in protein transport from the endoplasmic reticulum to the Golgi apparatus and from the Golgi apparatus and *trans*-Golgi network to the plasma membrane (18, 75). More recently, PKA has been reported to have a fundamental role in the polarized trafficking of apical proteins and lipids in the development of hepatic canalicular structures (52, 86, 98). H89, myrPKI, and Rp-cAMPS inhibition of PKA in HCV-infected Huh-7.5 cells reduced the infectivity of extracellular virus without modulating the level(s) of infectious virus or HCV RNA within the cell (Fig. 6B and 7B). H89 did not alter the amount of HCV RNA released from cells, suggesting that particle release is not affected. This is consistent with the observation that H89 treatment did not affect albumin secretion (Fig. 7C), suggesting that the general secretory pathway of the cells was not perturbed. Interestingly, FK treatment of HCV-infected cells in order to activate PKA (Fig. 10A) increased the infectivity of extracellular virus (Fig. 6E), suggesting that basal levels of PKA activity may limit extracellular virus infectivity.

To address how PKA modulates extracellular virus infectivity, it is important to consider the processes underlying HCV particle assembly and release. Recent data have highlighted the critical role of lipoprotein assembly and secretion in the HCV life cycle. The HCV core protein is an essential compo-

nent of particles, and association with lipid droplets is critical for the genesis of infectious particles (16, 74). Furthermore, the efficient release of particles from infected cells is reported to be dependent on VLDL assembly and secretion (19, 38, 50). The inhibition of PKA in naïve and HCV-infected Huh-7.5 cells reduced ApoB secretion by approximately 50% but had no effect on ApoE levels (Fig. 9A). However, the buoyant densities of particles released from H89-treated cells were comparable to those from untreated cells, suggesting that HCV particle association with lipoproteins is not regulated by PKA (Fig. 9B and C). This conclusion is further supported by the negligible effect(s) of PKA inhibitors on extracellular HCV RNA levels (Fig. 7A), in contrast to the previously reported inhibitory effect(s) of MTP inhibitors on both VLDL and HCV particle secretion (19, 38, 50).

In mammalian cells, PKA exists as two major isoforms, type I and type II, where PKAI localizes predominately in the cytoplasm and PKAII associates with cellular structures and organelles via AKAPs (89). Rp-cAMPS demonstrated a specific inhibition of HCV entry and infectious extracellular virus, whereas Rp-8-Br-cAMPS had no effect (Fig. 3A and 6D). To aid the interpretation of these results, we studied the PKA isoform specificity of the Rp analogs in Huh-7.5 cells using a recently developed BRET assay (29). Rp-8-Br-cAMPS specifically inhibited FK/IBMX-stimulated PKAI and not PKAII (Fig. 3B), suggesting a minimal involvement of PKAI in HCV infection.

FK treatment of Huh-7.5 cells stimulates PKAII but not PKAI (Fig. 3C), which may be attributable to their different subcellular locations. FK activates adenylyl cyclases at the plasma membrane and, in the absence of IBMX, PDEs will degrade cAMP before it reaches the intracellularly located PKAI. Rp-cAMPS had no effect on FK/IBMX-stimulated PKAII (Fig. 3B). However, treating cells with FK alone allowed us to demonstrate the specific inhibition of PKAII by Rp-cAMPS (Fig. 3C) and to confirm a role for PKAII in HCV infection.

PKAII is known to regulate diverse cellular functions due to its localization via AKAPs (22, 23, 100). GFP-AKAP-IS expression in Huh-7.5 cells was unstable, and we were unable to study HCV infection and viral protein trafficking in the *trans*-dominant-negative expressing cells. However, transient expression of AKAP-IS peptide, a specific AKAP disruptor of PKAII, in Huh-7.5 cells led to a relocalization of CLDN1 (Fig. 5C), confirming that PKA regulates CLDN1 targeting to the plasma membrane in an AKAP-dependent manner. Overall, our studies suggest a specific role for the PKAII isoform in the entry and infectivity of cell-free particles.

PKAII-AKAP interactions at the Golgi-centrosomal area (12, 101, 102) may coordinate lipid, cellular, and viral protein trafficking in Huh-7.5 cells. Thus, it is conceivable that inhibition of PKA may alter the passage of virus through the Golgi apparatus, resulting in the attenuation of its infectivity. HCV glycoproteins in the endoplasmic reticulum comprise high-mannose sugars, which are trimmed during their transit from the endoplasmic reticulum to the Golgi apparatus to complex type sugars (40). Experiments to determine the molecular weight and endoglycosidase sensitivity of extracellular particle-associated GPs yielded inconclusive data due to low viral yields. Helle and colleagues (45) reported that the neutralizing activity of anti-HCV antibodies was modulated by specific E2 glycans. Interestingly, cell-free virus released from control or H89-treated cells demonstrated sensitivities comparable to those obtained with neutralization by GP-specific monoclonal antibodies and patient IgG (data not shown), suggesting no major alteration(s) in the glycosylation status of particle-associated GPs released from treated cells.

We noted increased levels of cAMP and PKA substrates in infected cells (Fig. 10), supporting a model where HCV infection activates PKA in a cAMP-dependent manner as a mechanism to promote the infectivity of cell-free virus and viral transmission. Our evidence using HCVcc is in contrast to previous reports where the activity of PKA-C was inhibited with peptides corresponding to a sequence within the HCV NS3 region and recombinant NS3/NS4A (4, 15). Several examples exist, however, where viruses activate cAMP/PKA pathways, adenovirus activates PKA to enhance nuclear targeting via the microtubule network (94), and HIV infection is associated with increased levels of intracellular cAMP and constitutive PKA activation that are required for efficient proviral DNA synthesis (2, 47). Kim and colleagues reported that NS2 activated cAMP-dependent pathways in Huh-7 cells, supporting JFH-1 subgenomic replicons (55). Our data imaging PKA substrates in HCV-infected cells demonstrate colocalization with NS5A, suggesting that NS5A or other components of the viral replicase complex may be substrates for PKA (Fig. 10E). Experiments to investigate whether HCV particle interactions with cell surface receptors promote cAMP levels were inconclusive and may reflect low viral titers that fail to saturate cell surface-expressed receptors. Alternatively, the virus may induce cAMP-independent activation of PKA by second messenger lipids such as sphingosine (68) or via cross talk between signaling pathways. In addition, there may be endogenous PKA activity within the particle, as reported previously for hepatitis B virus, which encapsidates PKC into its core particle (53). In summary, we demonstrate a role for PKAII both in the infectivity of extracellular virus and in viral entry, highlighting potential new targets for therapy.

ACKNOWLEDGMENTS

We thank T. Wakita for JFH-1; C. M. Rice for J6/JFH, Huh-7.5 cells, and anti-NS5A 9E10; Adrian Thrasher for CSGW; P. Bieniasz for Gag-Pol plasmid; J. Scott for AKAP-IS and scrambled expression constructs; J. Lord for Rp-cAMPS and Rp-8-Br-cAMPS; and F. Berditchevski for anti-CD81 M38.

This work was supported by PHS grant AI50798, the MRC, and The Wellcome Trust. M.D. was supported by the Otto Braun Fond, and F.W.H. was supported by the European Union (LSHB-CT-2006-037189).

REFERENCES

1. **Alto, N. M., S. H. Soderling, N. Hoshi, L. K. Langeberg, R. Fayos, P. A. Jennings, and J. D. Scott.** 2003. Bioinformatic design of A-kinase anchoring protein-in silico: a potent and selective peptide antagonist of type II protein kinase A anchoring. Proc. Natl. Acad. Sci. USA **100:**4445–4450.
2. **Amella, C. A., B. Sherry, D. H. Shepp, and H. Schmidtmayerova.** 2005. Macrophage inflammatory protein 1α inhibits postentry steps of human immunodeficiency virus type 1 infection via suppression of intracellular cyclic AMP. J. Virol. **79:**5625–5631.
3. **Andrade, A. A., P. N. Silva, A. C. Pereira, L. P. De Sousa, P. C. Ferreira, R. T. Gazzinelli, E. G. Kroon, C. Ropert, and C. A. Bonjardim.** 2004. The vaccinia virus-stimulated mitogen-activated protein kinase (MAPK) pathway is required for virus multiplication. Biochem. J. **381:**437–446.
4. **Aoubala, M., J. Holt, R. A. Clegg, D. J. Rowlands, and M. Harris.** 2001. The inhibition of cAMP-dependent protein kinase by full-length hepatitis C

virus NS3/4A complex is due to ATP hydrolysis. J. Gen. Virol. **82:**1637–1646.
5. **Avila-Flores, A., E. Rendon-Huerta, J. Moreno, S. Islas, A. Betanzos, M. Robles-Flores, and L. Gonzalez-Mariscal.** 2001. Tight-junction protein zonula occludens 2 is a target of phosphorylation by protein kinase C. Biochem. J. **360:**295–304.
6. **Balda, M. S., L. Gonzalez-Mariscal, K. Matter, M. Cereijido, and J. M. Anderson.** 1993. Assembly of the tight junction: the role of diacylglycerol. J. Cell Biol. **123:**293–302.
7. **Bartenschlager, R., M. Frese, and T. Pietschmann.** 2004. Novel insights into hepatitis C virus replication and persistence. Adv. Virus Res. **63:**71–180.
8. **Bartosch, B., A. Vitelli, C. Granier, C. Goujon, J. Dubuisson, S. Pascale, E. Scarselli, R. Cortese, A. Nicosia, and F. L. Cosset.** 2003. Cell entry of hepatitis C virus requires a set of receptors that include the CD81 tetraspanin and the SR-B1 scavenger receptor. J. Biol. Chem. **278:**41624–41630.
9. **Berditchevski, F., K. F. Tolias, K. Wong, C. L. Carpenter, and M. E. Hemler.** 1997. A novel link between integrins, transmembrane-4 superfamily proteins (CD63 and CD81), and phosphatidylinositol 4-kinase. J. Biol. Chem. **272:**2595–2598.
10. **Berney, C., and G. Danuser.** 2003. FRET or no FRET: a quantitative comparison. Biophys. J. **84:**3992–4010.
11. **Besnier, C., L. Ylinen, B. Strange, A. Lister, Y. Takeuchi, S. P. Goff, and G. J. Towers.** 2003. Characterization of murine leukemia virus restriction in mammals. J. Virol. **77:**13403–13406.
12. **Birkeli, K. A., A. Llorente, M. L. Torgersen, G. Keryer, K. Tasken, and K. Sandvig.** 2003. Endosome-to-Golgi transport is regulated by protein kinase A type IIα. J. Biol. Chem. **278:**1991–1997.
13. **Blazev, R., M. Hussain, A. J. Bakker, S. I. Head, and G. D. Lamb.** 2001. Effects of the PKA inhibitor H-89 on excitation-contraction coupling in skinned and intact skeletal muscle fibres. J. Muscle Res. Cell Motil. **22:**277–286.
14. **Blight, K. J., J. A. McKeating, and C. M. Rice.** 2002. Highly permissive cell lines for subgenomic and genomic hepatitis C virus RNA replication. J. Virol. **76:**13001–13014.
15. **Borowski, P., K. Oehlmann, M. Heiland, and R. Laufs.** 1997. Nonstructural protein 3 of hepatitis C virus blocks the distribution of the free catalytic subunit of cyclic AMP-dependent protein kinase. J. Virol. **71:**2838–2843.
16. **Boulant, S., P. Targett-Adams, and J. McLauchlan.** 2007. Disrupting the association of hepatitis C virus core protein with lipid droplets correlates with a loss in production of infectious virus. J. Gen. Virol. **88:**2204–2213.
17. **Bruce, J. I., T. J. Shuttleworth, D. R. Giovannucci, and D. I. Yule.** 2002. Phosphorylation of inositol 1,4,5-trisphosphate receptors in parotid acinar cells. A mechanism for the synergistic effects of cAMP on Ca2+ signaling. J. Biol. Chem. **277:**1340–1348.
18. **Burgos, P. V., C. Klattenhoff, E. de la Fuente, A. Rigotti, and A. Gonzalez.** 2004. Cholesterol depletion induces PKA-mediated basolateral-to-apical transcytosis of the scavenger receptor class B type I in MDCK cells. Proc. Natl. Acad. Sci. USA **101:**3845–3850.
19. **Chang, K.-S., J. Jiang, Z. Cai, and G. Luo.** 2007. Human apolipoprotein E is required for infectivity and production of hepatitis C virus in cell culture. J. Virol. **81:**13783–13793.
20. **Chijiwa, T., A. Mishima, M. Hagiwara, M. Sano, K. Hayashi, T. Inoue, K. Naito, T. Toshioka, and H. Hidaka.** 1990. Inhibition of forskolin-induced neurite outgrowth and protein phosphorylation by a newly synthesized selective inhibitor of cyclic AMP-dependent protein kinase, N-[2-(p-bromocinnamylamino)ethyl]-5-isoquinolinesulfonamide (H-89), of PC12D pheochromocytoma cells. J. Biol. Chem. **265:**5267–5272.
21. **Cirone, M., A. Angeloni, G. Barile, C. Zompetta, M. Venanzoni, M. R. Torrisi, L. Frati, and A. Faggioni.** 1990. Epstein-Barr virus internalization and infectivity are blocked by selective protein kinase C inhibitors. Int. J. Cancer **45:**490–493.
22. **Coghlan, V. M., S. E. Bergeson, L. Langeberg, G. Nilaver, and J. D. Scott.** 1993. A-kinase anchoring proteins: a key to selective activation of cAMP-responsive events? Mol. Cell. Biochem. *127*-**128:**309–319.
23. **Colledge, M., and J. D. Scott.** 1999. AKAPs: from structure to function. Trends Cell Biol. **9:**216–221.
24. **Constantinescu, S. N., C. D. Cernescu, and L. M. Popescu.** 1991. Effects of protein kinase C inhibitors on viral entry and infectivity. FEBS Lett. **292:**31–33.
25. **Cook, L., K. W. Ng, A. Bagabag, L. Corey, and K. R. Jerome.** 2004. Use of the MagNA pure LC automated nucleic acid extraction system followed by real-time reverse transcription-PCR for ultrasensitive quantitation of hepatitis C virus RNA. J. Clin. Microbiol. **42:**4130–4136.
26. **Coyne, C. B., and J. M. Bergelson.** 2006. Virus-induced Abl and Fyn kinase signals permit coxsackievirus entry through epithelial tight junctions. Cell **124:**119–131.
27. **Davis, P. D., L. H. Elliott, W. Harris, C. H. Hill, S. A. Hurst, E. Keech, M. K. Kumar, G. Lawton, J. S. Nixon, and S. E. Wilkinson.** 1992. Inhibitors of protein kinase C. 2. Substituted bisindolylmaleimides with improved potency and selectivity. J. Med. Chem. **35:**994–1001.
28. **Delgrange, D., A. Pillez, S. Castelain, L. Cocquerel, Y. Rouille, J. Dubuisson, T. Wakita, G. Duverlie, and C. Wychowski.** 2007. Robust production of infectious viral particles in Huh-7 cells by introducing mutations in hepatitis C virus structural proteins. J. Gen. Virol. **88:**2495–2503.
29. **Diskar, M., H. M. Zenn, A. Kaupisch, A. Prinz, and F. W. Herberg.** 2007. Molecular basis for isoform-specific autoregulation of protein kinase A. Cell. Signal. **19:**2024–2034.
30. **Dostmann, W. R., S. S. Taylor, H. G. Genieser, B. Jastorff, S. O. Doskeland, and D. Ogreid.** 1990. Probing the cyclic nucleotide binding sites of cAMP-dependent protein kinases I and II with analogs of adenosine 3′,5′-cyclic phosphorothioates. J. Biol. Chem. **265:**10484–10491.
31. **D'Souza, T., R. Agarwal, and P. J. Morin.** 2005. Phosphorylation of claudin-3 at threonine 192 by cAMP-dependent protein kinase regulates tight junction barrier function in ovarian cancer cells. J. Biol. Chem. **280:**26233–26240.
32. **D'Souza, T., F. E. Indig, and P. J. Morin.** 2007. Phosphorylation of claudin-4 by PKCepsilon regulates tight junction barrier function in ovarian cancer cells. Exp. Cell Res. **313:**3364–3375.
33. **Dudley, D. T., L. Pang, S. J. Decker, A. J. Bridges, and A. R. Saltiel.** 1995. A synthetic inhibitor of the mitogen-activated protein kinase cascade. Proc. Natl. Acad. Sci. USA **92:**7686–7689.
34. **Evans, M. J., T. von Hahn, D. M. Tscherne, A. J. Syder, M. Panis, B. Wolk, T. Hatziioannou, J. A. McKeating, P. D. Bieniasz, and C. M. Rice.** 2007. Claudin-1 is a hepatitis C virus co-receptor required for a late step in entry. Nature **446:**801–805.
35. **Favata, M. F., K. Y. Horiuchi, E. J. Manos, A. J. Daulerio, D. A. Stradley, W. S. Feeser, D. E. Van Dyk, W. J. Pitts, R. A. Earl, F. Hobbs, R. A. Copeland, R. L. Magolda, P. A. Scherle, and J. M. Trzaskos.** 1998. Identification of a novel inhibitor of mitogen-activated protein kinase kinase. J. Biol. Chem. **273:**18623–18632.
36. **Flint, M., T. von Hahn, J. Zhang, M. Farquhar, C. T. Jones, P. Balfe, C. M. Rice, and J. A. McKeating.** 2006. Diverse CD81 proteins support hepatitis C virus infection. J. Virol. **80:**11331–11342.
37. **Fujibe, M., H. Chiba, T. Kojima, T. Soma, T. Wada, T. Yamashita, and N. Sawada.** 2004. Thr203 of claudin-1, a putative phosphorylation site for MAP kinase, is required to promote the barrier function of tight junctions. Exp. Cell Res. **295:**36–47.
38. **Gastaminza, P., G. Cheng, S. Wieland, J. Zhong, W. Liao, and F. V. Chisari.** 2008. Cellular determinants of hepatitis C virus assembly, maturation, degradation, and secretion. J. Virol. **82:**2120–2129.
39. **Gjertsen, B. T., G. Mellgren, A. Otten, E. Maronde, H. G. Genieser, B. Jastorff, O. K. Vintermyr, G. S. McKnight, and S. O. Doskeland.** 1995. Novel (Rp)-cAMPS analogs as tools for inhibition of cAMP-kinase in cell culture. Basal cAMP-kinase activity modulates interleukin-1β action. J. Biol. Chem. **270:**20599–20607.
40. **Goffard, A., and J. Dubuisson.** 2003. Glycosylation of hepatitis C virus envelope proteins. Biochimie **85:**295–301.
41. **Grove, J., T. Huby, Z. Stamataki, T. Vanwolleghem, P. Meuleman, M. Farquhar, A. Schwarz, M. Moreau, J. S. Owen, G. Leroux-Roels, P. Balfe, and J. A. McKeating.** 2007. Scavenger receptor BI and BII expression levels modulate hepatitis C virus infectivity. J. Virol. **81:**3162–3169.
42. **Hachet-Haas, M., N. Converset, O. Marcha, H. Matthes, S. Gioria, J.-L. Galzi, and S. Lecat.** 2006. FRET and colocalization analyzer—a method to validate measurements of sensitized emission FRET acquired by confocal microscopy and available as an ImageJ plug-in. Microsc. Res. Tech. **69:**941–956.
43. **Harris, H. J., M. J. Farquhar, C. J. Mee, C. Davis, G. M. Reynolds, A. Jennings, K. Hu, F. Yuan, H. Deng, S. G. Hubscher, J. H. Han, P. Balfe, and J. A. McKeating.** 2008. CD81 and claudin 1 coreceptor association: role in hepatitis C virus entry. J. Virol. **82:**5007–5020.
44. **Harris, T. E., S. J. Persaud, and P. M. Jones.** 1997. Pseudosubstrate inhibition of cyclic AMP-dependent protein kinase in intact pancreatic islets: effects on cyclic AMP-dependent and glucose-dependent insulin secretion. Biochem. Biophys. Res. Commun. **232:**648–651.
45. **Helle, F., A. Goffard, V. Morel, G. Duverlie, J. McKeating, Z. Y. Keck, S. Foung, F. Penin, J. Dubuisson, and C. Voisset.** 2007. The neutralizing activity of anti-hepatitis C virus antibodies is modulated by specific glycans on the E2 envelope protein. J. Virol. **81:**8101–8111.
46. **Herberg, F. W., and S. S. Taylor.** 1993. Physiological inhibitors of the catalytic subunit of cAMP-dependent protein kinase: effect of MgATP on protein-protein interactions. Biochemistry **32:**14015–14022.
47. **Hofmann, B., P. Nishanian, T. Nguyen, M. Liu, and J. L. Fahey.** 1993. Restoration of T-cell function in HIV infection by reduction of intracellular cAMP levels with adenosine analogues. AIDS **7:**659–664.
48. **Howl, J., R. M. Mondszein, and M. Wheatley.** 1998. Characterization of G protein-coupled receptors expressed by ECV304 human endothelial cells. Endothelium **6:**23–32.
49. **Hsu, M., J. Zhang, M. Flint, C. Logvinoff, C. Cheng-Mayer, C. M. Rice, and J. A. McKeating.** 2003. Hepatitis C virus glycoproteins mediate pH-dependent cell entry of pseudotyped retroviral particles. Proc. Natl. Acad. Sci. USA **100:**7271–7276.
50. **Huang, H., F. Sun, D. M. Owen, W. Li, Y. Chen, M. Gale, Jr., and J. Ye.**

2007. Hepatitis C virus production by human hepatocytes dependent on assembly and secretion of very low-density lipoproteins. Proc. Natl. Acad. Sci. USA **104:**5848–5853.
51. **Ikari, A., M. Ito, C. Okude, H. Sawada, H. Harada, M. Degawa, H. Sakai, T. Takahashi, J. Sugatani, and M. Miwa.** 2007. Claudin-16 is directly phosphorylated by protein kinase A independently of a vasodilator-stimulated phosphoprotein-mediated pathway. J. Cell. Physiol. **214:**221–229.
52. **Kagawa, T., L. Varticovski, Y. Sai, and I. M. Arias.** 2002. Mechanism by which cAMP activates PI3-kinase and increases bile acid secretion in WIF-B9 cells. Am. J. Physiol. Cell Physiol. **283:**C1655–C1666.
53. **Kann, M., R. Thomssen, H. G. Kochel, and W. H. Gerlich.** 1993. Characterization of the endogenous protein kinase activity of the hepatitis B virus. Arch. Virol. Suppl. **8:**53–62.
54. **Kemp, B. E., R. B. Pearson, and C. M. House.** 1991. Pseudosubstrate-based peptide inhibitors. Methods Enzymol. **201:**287–304.
55. **Kim, K. M., S. N. Kwon, J. I. Kang, S. H. Lee, S. K. Jang, B. Y. Ahn, and Y. K. Kim.** 2007. Hepatitis C virus NS2 protein activates cellular cyclic AMP-dependent pathways. Biochem. Biophys. Res. Commun. **356:**948–954.
56. **Kim, S. K., K. J. Woodcroft, S. S. Khodadadeh, and R. F. Novak.** 2004. Insulin signaling regulates gamma-glutamylcysteine ligase catalytic subunit expression in primary cultured rat hepatocytes. J. Pharmacol. Exp. Ther. **311:**99–108.
57. **Kohler, K., D. Louvard, and A. Zahraoui.** 2004. Rab13 regulates PKA signaling during tight junction assembly. J. Cell Biol. **165:**175–180.
58. **Kohler, K., and A. Zahraoui.** 2005. Tight junction: a co-ordinator of cell signalling and membrane trafficking. Biol. Cell **97:**659–665.
59. **Lehmann, M. J., N. M. Sherer, C. B. Marks, M. Pypaert, and W. Mothes.** 2005. Actin- and myosin-driven movement of viruses along filopodia precedes their entry into cells. J. Cell Biol. **170:**317–325.
60. **Levy, S., and T. Shoham.** 2005. The tetraspanin web modulates immune-signalling complexes. Nat. Rev. Immunol. **5:**136–148.
61. **Li, X., E. Huston, M. J. Lynch, M. D. Houslay, and G. S. Baillie.** 2006. Phosphodiesterase-4 influences the PKA phosphorylation status and membrane translocation of G-protein receptor kinase 2 (GRK2) in HEK-293β2 cells and cardiac myocytes. Biochem. J. **394:**427–435.
62. **Lin, D., A. S. Edwards, J. P. Fawcett, G. Mbamalu, J. D. Scott, and T. Pawson.** 2000. A mammalian PAR-3-PAR-6 complex implicated in Cdc42/Rac1 and aPKC signalling and cell polarity. Nat. Cell Biol. **2:**540–547.
63. **Lindenbach, B. D., M. J. Evans, A. J. Syder, B. Wolk, T. L. Tellinghuisen, C. C. Liu, T. Maruyama, R. O. Hynes, D. R. Burton, J. A. McKeating, and C. M. Rice.** 2005. Complete replication of hepatitis C virus in cell culture. Science **309:**623–626.
64. **Lindenbach, B. D., P. Meuleman, A. Ploss, T. Vanwolleghem, A. J. Syder, J. A. McKeating, R. E. Lanford, S. M. Feinstone, M. E. Major, G. Leroux-Roels, and C. M. Rice.** 2006. Cell culture-grown hepatitis C virus is infectious in vivo and can be recultured in vitro. Proc. Natl. Acad. Sci. USA **103:**3805–3809.
65. **Lochner, A., and J. A. Moolman.** 2006. The many faces of H89: a review. Cardiovasc. Drug Rev. **24:**261–274.
66. **Lokshin, A., T. Raskovalova, X. Huang, L. C. Zacharia, E. K. Jackson, and E. Gorelik.** 2006. Adenosine-mediated inhibition of the cytotoxic activity and cytokine production by activated natural killer cells. Cancer Res. **66:**7758–7765.
67. **Lu, W., and J. H. Ou.** 2002. Phosphorylation of hepatitis C virus core protein by protein kinase A and protein kinase C. Virology **300:**20–30.
68. **Ma, Y., S. Pitson, T. Hercus, J. Murphy, A. Lopez, and J. Woodcock.** 2005. Sphingosine activates protein kinase A type II by a novel cAMP-independent mechanism. J. Biol. Chem. **280:**26011–26017.
69. **Machado, J. D., A. Morales, J. F. Gomez, and R. Borges.** 2001. cAmp modulates exocytotic kinetics and increases quantal size in chromaffin cells. Mol. Pharmacol. **60:**514–520.
70. **Matsuda, M., A. Kubo, M. Furuse, and S. Tsukita.** 2004. A peculiar internalization of claudins, tight junction-specific adhesion molecules, during the intercellular movement of epithelial cells. J. Cell Sci. **117:**1247–1257.
71. **Mee, C. J., J. Grove, H. J. Harris, K. Hu, P. Balfe, and J. A. McKeating.** 2008. Effect of cell polarization on hepatitis C virus entry. J. Virol. **82:**461–470.
72. **Meertens, L., C. Bertaux, L. Cukierman, E. Cormier, D. Lavillette, F.-L. Cosset, and T. Dragic.** 2008. The tight junction proteins claudin-1, -6, and -9 are entry cofactors for the hepatitis C virus. J. Virol. **82:**3555–3560.
73. **Meuleman, P., L. Libbrecht, R. De Vos, B. de Hemptinne, K. Gevaert, J. Vandekerckhove, T. Roskams, and G. Leroux-Roels.** 2005. Morphological and biochemical characterization of a human liver in a uPA-SCID mouse chimera. Hepatology **41:**847–856.
74. **Miyanari, Y., K. Atsuzawa, N. Usuda, K. Watashi, T. Hishiki, M. Zayas, R. Bartenschlager, T. Wakita, M. Hijikata, and K. Shimotohno.** 2007. The lipid droplet is an important organelle for hepatitis C virus production. Nat. Cell Biol. **9:**1089–1097.
75. **Muniz, M., M. Alonso, J. Hidalgo, and A. Velasco.** 1996. A regulatory role for cAMP-dependent protein kinase in protein traffic along the exocytic route. J. Biol. Chem. **271:**30935–30941.
76. **Murray, J. L., M. Mavrakis, N. J. McDonald, M. Yilla, J. Sheng, W. J. Bellini, L. Zhao, J. M. Le Doux, M. W. Shaw, C. C. Luo, J. Lippincott-Schwartz, A. Sanchez, D. H. Rubin, and T. W. Hodge.** 2005. Rab9 GTPase is required for replication of human immunodeficiency virus type 1, filoviruses, and measles virus. J. Virol. **79:**11742–11751.
77. **Nakamura, T., N. Shibata, T. Nishimoto-Shibata, D. Feng, M. Ikemoto, K. Motojima, O. N. Iso, K. Tsukamoto, M. Tsujimoto, and H. Arai.** 2005. Regulation of SR-BI protein levels by phosphorylation of its associated protein, PDZK1. Proc. Natl. Acad. Sci. USA **102:**13404–13409.
78. **Nielsen, S. U., M. F. Bassendine, A. D. Burt, C. Martin, W. Pumeechockchai, and G. L. Toms.** 2006. Association between hepatitis C virus and very-low-density lipoprotein (VLDL)/LDL analyzed in iodixanol density gradients. J. Virol. **80:**2418–2428.
79. **Parent, A. T., N. Y. Barnes, Y. Taniguchi, G. Thinakaran, and S. S. Sisodia.** 2005. Presenilin attenuates receptor-mediated signaling and synaptic function. J. Neurosci. **25:**1540–1549.
80. **Pelkmans, L., E. Fava, H. Grabner, M. Hannus, B. Habermann, E. Krausz, and M. Zerial.** 2005. Genome-wide analysis of human kinases in clathrin- and caveolae/raft-mediated endocytosis. Nature **436:**78–86.
81. **Pichard, L., E. Raulet, G. Fabre, J. B. Ferrini, J. C. Ourlin, and P. Maurel.** 2006. Human hepatocyte culture. Methods Mol. Biol. **320:**283–293.
82. **Pileri, P., Y. Uematsu, S. Campagnoli, G. Galli, F. Falugi, R. Petracca, A. J. Weiner, M. Houghton, D. Rosa, G. Grandi, and S. Abrignani.** 1998. Binding of hepatitis C virus to CD81. Science **282:**938–941.
83. **Prinz, A., M. Diskar, A. Erlbruch, and F. W. Herberg.** 2006. Novel, isotype-specific sensors for protein kinase A subunit interaction based on bioluminescence resonance energy transfer (BRET). Cell. Signal. **18:**1616–1625.
84. **Prinz, A., M. Diskar, and F. W. Herberg.** 2006. Application of bioluminescence resonance energy transfer (BRET) for biomolecular interaction studies. Chembiochem **7:**1007–1012.
85. **Rabbi, M. F., L. al-Harthi, M. Saifuddin, and K. A. Roebuck.** 1998. The cAMP-dependent protein kinase A and protein kinase C-β pathways synergistically interact to activate HIV-1 transcription in latently infected cells of monocyte/macrophage lineage. Virology **245:**257–269.
86. **Roma, M. G., P. Milkiewicz, E. Elias, and R. Coleman.** 2000. Control by signaling modulators of the sorting of canalicular transporters in rat hepatocyte couplets: role of the cytoskeleton. Hepatology **32:**1342–1356.
87. **Root, C. N., E. G. Wills, L. L. McNair, and G. R. Whittaker.** 2000. Entry of influenza viruses into cells is inhibited by a highly specific protein kinase C inhibitor. J. Gen. Virol. **81:**2697–2705.
88. **Scarselli, E., H. Ansuini, R. Cerino, R. M. Roccasecca, S. Acali, G. Filocamo, C. Traboni, A. Nicosia, R. Cortese, and A. Vitelli.** 2002. The human scavenger receptor class B type I is a novel candidate receptor for the hepatitis C virus. EMBO J. **21:**5017–5025.
89. **Scott, J. D.** 1991. Cyclic nucleotide-dependent protein kinases. Pharmacol. Ther. **50:**123–145.
90. **Seino, S., and T. Shibasaki.** 2005. PKA-dependent and PKA-independent pathways for cAMP-regulated exocytosis. Physiol. Rev. **85:**1303–1342.
91. **Sieczkarski, S. B., H. A. Brown, and G. R. Whittaker.** 2003. Role of protein kinase C βII in influenza virus entry via late endosomes. J. Virol. **77:**460–469.
92. **Singh, A. B., and R. C. Harris.** 2004. Epidermal growth factor receptor activation differentially regulates claudin expression and enhances transepithelial resistance in Madin-Darby canine kidney cells. J. Biol. Chem. **279:**3543–3552.
93. **Suomalainen, M., M. Y. Nakano, K. Boucke, S. Keller, and U. F. Greber.** 2001. Adenovirus-activated PKA and p38/MAPK pathways boost microtubule-mediated nuclear targeting of virus. EMBO J. **20:**1310–1319.
94. **Tanaka, M., R. Kamata, and R. Sakai.** 2005. EphA2 phosphorylates the cytoplasmic tail of claudin-4 and mediates paracellular permeability. J. Biol. Chem. **280:**42375–42382.
95. **Tang, Y., S. E. Sefers, and H. J. Li.** 2005. Primer sequence modification enhances hepatitis C virus genotype coverage. J. Clin. Microbiol. **43:**3576–3577.
96. **Tasken, K., and E. M. Aandahl.** 2004. Localized effects of cAMP mediated by distinct routes of protein kinase A. Physiol. Rev. **84:**137–167.
97. **van IJzendoorn, S. C. D., and D. Hoekstra.** 2000. Polarized sphingolipid transport from the subapical compartment changes during cell polarity development. Mol. Biol. Cell **11:**1093–1101.
98. **van IJzendoorn. S. C. D., and D. Hoekstra.** 1999. Polarized sphingolipid transport from the subapical compartment: evidence for distinct sphingolipid domains. Mol. Biol. Cell **10:**3449–3461.
99. **Wakita, T., T. Pietschmann, T. Kato, T. Date, M. Miyamoto, Z. Zhao, K. Murthy, A. Habermann, H. G. Krausslich, M. Mizokami, R. Bartenschlager, and T. J. Liang.** 2005. Production of infectious hepatitis C virus in tissue culture from a cloned viral genome. Nat. Med. **11:**791–796.
100. **Wojtal, K. A., E. de Vries, D. Hoekstra, and S. C. D. van IJzendoorn.** 2006. Efficient trafficking of MDR1/P-glycoprotein to apical canalicular plasma membranes in HepG2 cells requires PKA-RIIalpha anchoring and glucosylceramide. Mol. Biol. Cell **17:**3638–3650.
101. **Wojtal, K. A., D. Hoekstra, and S. C. D. van Ijzendoorn.** 2007. Anchoring of protein kinase A-regulatory subunit IIα to subapically positioned cen-

trosomes mediates apical bile canalicular lumen development in response to oncostatin M but not cAMP. Mol. Biol. Cell **18:**2745–2754.

102. **Wojtal, K. A., D. Hoekstra, and S. C. D. van Ijzendoorn.** 2008. cAMP-dependent protein kinase A and the dynamics of epithelial cell surface domains: moving membranes to keep in shape. Bioessays **30:**146–155.
103. **Xia, K., D. M. Knipe, and N. A. DeLuca.** 1996. Role of protein kinase A and the serine-rich region of herpes simplex virus type 1 ICP4 in viral replication. J. Virol. **70:**1050–1060.
104. **Yang, W., C. Qiu, N. Biswas, J. Jin, S. C. Watkins, R. C. Montelaro, C. B. Coyne, and T. Wang.** 2008. Correlation of the tight junction-like distribution of claudin-1 to the cellular tropism of HCV. J. Biol. Chem. **283:**8643–8653.
105. **Zal, T., and N. R. Gascoigne.** 2004. Photobleaching-corrected FRET efficiency imaging of live cells. Biophys. J. **86:**3923–3939.
106. **Zegers, M. M., and D. Hoekstra.** 1997. Sphingolipid transport to the apical plasma membrane domain in human hepatoma cells is controlled by PKC and PKA activity: a correlation with cell polarity in HepG2 cells. J. Cell Biol. **138:**307–321.
107. **Zhang, J., G. Randall, A. Higginbottom, P. Monk, C. M. Rice, and J. A. McKeating.** 2004. CD81 is required for hepatitis C virus glycoprotein-mediated viral infection. J. Virol. **78:**1448–1455.
108. **Zhang, X. A., A. L. Bontrager, and M. E. Hemler.** 2001. Transmembrane-4 superfamily proteins associate with activated protein kinase C (PKC) and link PKC to specific β(1) integrins. J. Biol. Chem. **276:**25005–25013.
109. **Zheng, A., F. Yuan, Y. Li, F. Zhu, P. Hou, J. Li, X. Song, M. Ding, and H. Deng.** 2007. Claudin-6 and claudin-9 function as additional coreceptors for hepatitis C virus. J. Virol. **81:**12465–12471.
110. **Zhong, J., P. Gastaminza, G. Cheng, S. Kapadia, T. Kato, D. R. Burton, S. F. Wieland, S. L. Uprichard, T. Wakita, and F. V. Chisari.** 2005. Robust hepatitis C virus infection in vitro. Proc. Natl. Acad. Sci. USA **102:**9294–9299.